MATHEMATISCHES FORSCHUNGSINSTITUT OBERWOLFACH

Mini-Workshop: Numerical Upscaling for Media with Deterministic and Stochastic Heterogeneity

Organised by
Yalchin Efendiev, College Station
Oleg Iliev, Kaiserslautern
Panayot Vassilevski, Livermore

10 February – 16 February 2013

ABSTRACT. This minisymposium was third in series of similar events, after two very successful meetings in 2005 and 2009. The aim was to provide a forum for an extensive discussion on the theoretical aspects and on the areas of application and validity of numerical upscaling approaches for heterogeneous problems with deterministic and stochastic coefficients. The intensive discussions during the meeting contributed to a better understanding of upscaling approaches for multiscale problems with stochastic coefficients, and for synergy between scientists coming to this topic from the area of deterministic multiscale problems on one hand, and those coming from the area of SPDE on the other hand. Recent advanced results on upscaling approaches for deterministic multiscale problems were presented, well mixed with strong presentations on SDE and SPDE. The open problems in these areas were discussed, with emphasis on the case of stochastic coefficients brainstorming numerous numerical upscaling approaches. A number of young researchers, very actively working in these areas, were involved in the workshop discussing the links between scales., thus ensuring the continuity between the generations of researchers.

Mathematics Subject Classification (2010): 65, 68, 70, 74, 76.

Introduction by the Organisers

1. AIM AND MOTIVATION

This minisymposium was third in series of similar events. The previous two minisymposia on Numerical Upscaling took place in 2005 and 2009 and were very successful. In particular, the last one, in 2009, concentrated on differences and

similarities of FE/FV based numerical methods for multiscale problems from one side, and algebraic multigrid methods for the same problems, from another side. The intensive discussions on the common points between these two approaches allowed identifying the topics for synergetic developments. Further on, there was a second core of the discussions there, and this was the synergy between developing method for upscaling multiscale problems, and developing robust multilevel preconditioners for multiscale problems.

The aim of the third mini-workshop, held in 2013, was to provide a forum for an extensive discussion on the theoretical aspects and on the areas of application and validity of numerical upscaling approaches for heterogeneous problems with deterministic and stochastic coefficients. The term "numerical upscaling" is used here to denote several approaches (to be discussed below) for studying multiscale problems in the case when the scales cannot be separated (e.g., heterogeneity exist at each scale and the asymptotic homogenization is not directly applicable). The uncertainty discussed, concerns stochastic elliptic PDEs and systems of PDEs. A recapitulation of the achievements on upscaling approaches for deterministic multiscale problems was done, accompanied by intensive discussion on the open problems in the area. Strong presentations on SDE and SPDE allowed to better understand the specifics of these problems. Brainstorming on numerical upscaling approaches for the case of stochastic coefficients was among the main goals of the meeting.

2. Background

Multiscale problems, due to their importance for many branches of science and industry, attract significant attention of the mathematical community. Essential success was achieved during the last decades in the studies of problems with clearly separated fine and coarse scales (e.g., periodic microstructures, which are heterogeneous at a fine scale, but are homogeneous at a coarse scale). In this case the ratio between the fine and the coarse scale can play the role of a small parameter, and asymptotical analysis can be performed. Rigorous results were obtained in the field of (asymptotic) homogenization.

However, many scientific and industrial multiscale problems do not fall into the category of problems with scale separation. Intensive research on variety of numerical upscaling approaches was carried out in the last decade. At the same time, the Algebraic Multigrid Methods also evolved in this direction. The most active mathematical research in the field of numerical upscaling for flow problems is currently carried out in three directions: upscaling based on multigrid methods, upscaling based on multiscale finite element method and related approaches (MSFV, HMM, Variational Multiscale Method, etc.), and application of upscaling for solving multiscale industrial and environmental problems. Both, MG and multiscale FEM, provide a suitable framework for solving multiscale problems in the case of no scale separation. A number of papers devoted to multigrid and upscaling were published recently. A topic, related to both, AMG and multiscale FEM, is the so called Algebraic Multigrid-element method, AMGe. Methods like

Multiscale FEM, MsFEM; Multiscale Finite Volume, MSFV; Variational Multiscale Method; Heterogeneous Multiscale Method, are well understood now, at least when applied as numerical upscaling procedure for multiscale linear elliptic problems. Complementary to this, some of these methods became a popular choice as an ingredient of two level domain decomposition preconditioners for heterogeneous problems. The consecutive iterations fine-to-coarse and coarse-to-fine scale is a natural feature of the multigrid method. In the last decade it was shown that approaches like model reduction has a great potential for solving multiscale problems. Intensive research is carried out recently in the area of multiscale stochastic PDE. This include both, stochastic homogenization and numerical upscaling for SPDE. Researchers from most of these closely related directions were invited to participate in the discussions.

3. Topics

The discussion was restricted to continuous-to-continuous upscaling for elliptic problems with deterministic and stochastic coefficients. Scalar PDEs as well as systems of PDEs were considered. The field of numerical upscaling is still a very broad research field, and for the miniworkshop several well focused topics were defined.

- *Numerical upscaling approaches.* MsFEM, MSFV, VMS, Heterogeneous Multiscale Method, etc. versus AMG, AMGe, EMB, etc. Multilevel/Multigrid preconditioners for multiscale problems; Frameworks for solving multiscale problems: Similarities, differences and synergy.
- *Numerical upscaling approaches for stochastic multiscale problems*: what can be reused from deterministic numerical upscaling approaches? Reduced basis approaches for deterministic and stochastic multiscale problems. Multlevel approaches for stochastic problems.
- *Upscaling effective properties of heterogeneous media in the case of stochastic media.* Spectral methods versus Monte Carlo and Multilevel Monte Carlo: robustness, efficiency, etc.
- *Convergence results.* A priori and a posteriori estimates for deterministic problems. How to use a posteriori estimates for developing adaptive multilevel precondiotioners for multiscale problems. Convergence of the spectral methods and Monte Carlo type methods in the case of multiscale problems with stochastic coefficients.
- *Benchmarking and validation.* A careful specification of benchmark problems and validation approaches is needed in the field of numerical upscaling. A class of benchmark problems can be provided by asymptotic homogenization, when the latter is applicable. Defining benchmark tests for coupled multiscale problems with deterministic and stochastic coefficients will be discussed.

The thorough and concentrated consideration of the above topics by the qualified participants in the mini-workshop ensured a strong synergy effect. Interconnections between different approaches were identified, thus enriching each of them, and providing a background for new developments.

Mini-Workshop: Numerical Upscaling for Media with Deterministic and Stochastic Heterogeneity

Table of Contents

Abstracts

Data sparse approximation of the Karhunen-Loève expansion
ALEXANDER LITVINENKO
(joint work with Boris Khoromskij, Hermann G. Matthies)

1. INTRODUCTION

To approximate a random field $\kappa(x,\omega)$ with as few random variables as possible, but still retaining the essential information, the Karhunen-Loève expansion (KLE) becomes important. Often the random field is characterised by its covariance function $\text{cov}_\kappa(x,y)$. The KLE of a random field requires the solution of eigenvalue problem with the integral operator which has the covariance matrix as its kernel. Usually this eigenvalue problem is solved by a Krylov subspace method with a sparse matrix approximation. We demonstrate the use of the sparse hierarchical matrix ($\mathcal{H}$-matrix) technique with a log-linear computational cost of the matrix-vector product and a log-linear storage requirement.

Let us define the following operator T which will be needed for computing the KLE of $\kappa(x,\omega)$:

$$T : L^2(\mathcal{G}) \to L^2(\mathcal{G}), \quad (Tv)(x) := \int_{\mathcal{G}} \text{cov}_\kappa(x,y)v(y)\mathrm{d}y,$$

where $\mathcal{G}$ is a computational domain. For $\text{cov}_\kappa \in L^2(\mathcal{G} \times \mathcal{G})$ the operator T is compact and selfadjoint, in fact, Hilbert-Schmidt. As the covariance function cov_κ is symmetric positive definite, hence so is T [1]. Thus, the eigenfunctions v_ℓ of the following Fredholm integral equation of the second kind

$$(1) \qquad\qquad Tv_\ell = \lambda_\ell v_\ell, \quad v_\ell \in L^2(\mathcal{G}), \quad \ell \in \mathbb{N},$$

are mutually orthogonal and define a basis of $L^2(\mathcal{G})$. The eigenvalues λ_ℓ are real, non-negative and can be arranged decreasingly $\lambda_1 \geq \lambda_2 \geq ... \geq 0$. By definition, the KLE of $\kappa(x,\omega)$ is the following series

$$(2) \qquad\qquad \kappa(x,\omega) = E_\kappa(x) + \sum_{\ell=1}^{\infty} \sqrt{\lambda_\ell}v_\ell(x)\xi_\ell(\omega),$$

where $E_\kappa(x)$ is the mean value of $\kappa(x,\omega)$, λ_ℓ and v_ℓ are the eigenvalues/eigenvectors of the operator T and $\xi_\ell(\omega)$ are uncorrelated random variables. For numerical purposes one truncates the KLE (2) to a finite number m of terms. In the case of a Gaussian random field, the ξ_ℓ are independent standard normal random variables.

2. FE DISCRETISATION OF EQUATION (1) AND NUMERICS

In general, the eigenvalue problem (1) needs to be solved numerically and standard techniques may be used for this purpose. Assume that $b_1,...,b_N$ are the nodal basis functions with respect to the nodes $x_1,...,x_N \in \mathcal{G} \subset \mathbb{R}^d$, i.e. $b_i(x_j) = \delta_{ij}$, $i,j \in I$, $I = \{1,...,N\}$. The discrete eigenvalue problem will be as follows

$$\mathbf{MCMv}_\ell = \lambda_\ell \mathbf{Mv}_\ell, \quad \mathbf{C}_{ij} = \mathrm{cov}_\kappa(x_i, x_j), \quad \mathbf{M}_{ij} = \int_\mathcal{G} b_i(x)b_j(x)\mathrm{d}x, \quad i,j,\ell \in I.$$

Recall that the matrix $\mathbf{C}$ is symmetric positive definite and dense. The mass matrix $\mathbf{M}$ is symmetric positive definite and may be sparse. Typical examples of the covariance function are a) $\mathrm{cov}(\rho) = \exp\{-\rho^2\}$ (Gaussian type) and b) $\mathrm{cov}(\rho) = \exp\{-\rho\}$ (exponential type), where $\rho(x_i, x_j) = \sqrt{\sum_{\nu=1}^d \left(x_i^{(\nu)} - x_j^{(\nu)}\right)^2 / l_\nu^2}$, l_ν are correlation length scales, $x_i = \left(x_i^{(1)},...,x_i^{(d)}\right)$ and $x_j = \left(x_j^{(1)},...,x_j^{(d)}\right) \in \mathcal{G}$, $d = 2,3$. We approximate $\mathbf{C}$ in the $\mathcal{H}$-matrix format [1] with the cost $\mathcal{O}(kN\log N)$, where k is the maximal rank of subblocks. To compute m eigenvalues ($m \ll N$) (see Table 2) and the corresponding eigenvectors we apply an iterative Krylov subspace (Lanczos) eigenvalue solver. An $\mathcal{H}$-matrix approximation $\tilde{\mathbf{C}}$ consists of low-rank blocks and dense blocks. All low-rank blocks are computed by the adaptive cross approximation algorithm (ACA) [1].

All the following numerical experiments are done on PC with a 2GHz processor and with 3GB RAM (see more in [1, 2]). The first table shows that the computing time and memory requirements for the $\mathcal{H}$-matrix approximation $\tilde{\mathbf{C}}$ are much smaller than for the dense matrix $\mathbf{C}$.

N	rank k of $\tilde{\mathbf{C}}$	size, MB		t, sec.		$\frac{\|(\mathbf{C}-\tilde{\mathbf{C}})\mathbf{z}\|_2}{\|\mathbf{C}\|_2\|\mathbf{z}\|_2}$	$\max_{i=1..10} \|\lambda_i - \tilde{\lambda}_i\|$	$\frac{\|\|\mathbf{C}\|_2 - \|\tilde{\mathbf{C}}\|_2\|}{\|\mathbf{C}\|_2}$
		$\mathbf{C}$	$\tilde{\mathbf{C}}$	$\mathbf{C}$	$\tilde{\mathbf{C}}$			
$4.0 \cdot 10^3$	10	48	3	0.8	0.08	$7 \cdot 10^{-3}$	$7.0 \cdot 10^{-2}$	$2.0 \cdot 10^{-4}$
$1.05 \cdot 10^4$	18	439	19	7.0	0.4	$7 \cdot 10^{-4}$	$5.5 \cdot 10^{-2}$	$1.0 \cdot 10^{-4}$
$2.1 \cdot 10^4$	25	2054	64	45.0	1.4	$1 \cdot 10^{-5}$	$5.0 \cdot 10^{-2}$	$4.4 \cdot 10^{-6}$

TABLE 1. $\mathcal{H}$-matrix approximation of the covariance function of the exponential type, $l_1 = l_3 = 0.1$, $l_2 = 0.5$, $\mathcal{G}$ is 3D L-shape domain [1, 2]), $\mathbf{z}$ is a random vector.

Table 3 demonstrates the accuracy of the $\mathcal{H}$-matrix approximation of the covariance function of the exponential type for different covariance lengths l_1 and l_2 ($\mathcal{G} = [0,1]^2$, $n = 129^2$).

For small problem sizes such as 33^2, 65^2 (in 2D) it is possible to compute the exact covariance matrix $\mathbf{C}$ and check the accuracy of the $\mathcal{H}$-matrix approximation (the last column of Tab. 4), but for large problem sizes there is not enough memory ("nem") to store the matrix $\mathbf{C}$.

For a stationary covariance function (i.e. $\mathrm{cov}(x,y) = \mathrm{cov}(|x - y|)$) and a rectangular computational domain with tensor grid, the Fast Fourier technique (FFT)

matrix info (MB, sec.)				m					
N	k	size of $\tilde{\mathbf{C}}$	time to set up $\tilde{\mathbf{C}}$	2	5	10	20	40	80
$2.4 \cdot 10^4$	4	12	0.2	0.6	0.9	1.3	2.3	4.2	8
$6.8 \cdot 10^4$	8	95	2	2.4	3.8	5.6	8.4	18.0	28
$2.3 \cdot 10^5$	12	570	11	10.0	17.0	24.0	39.0	70.0	150

TABLE 2. Time required for computing m eigenpairs of the covariance function of the exponential type with $l_1 = l_3 = 0.1$, $l_2 = 0.5$ for L-shape 3D domain with the edge size 1.

l_1	l_2	ε
0.01	0.02	$3 \cdot 10^{-2}$
0.1	0.2	$8 \cdot 10^{-3}$
0.5	1	$2.8 \cdot 10^{-5}$

TABLE 3. Dependence of the $\mathcal{H}$-matrix accuracy on the covariance lengths l_1 and l_2.

n	time (sec.)		memory (MB)		
	$\mathbf{C}$	$\tilde{\mathbf{C}}$	$\mathbf{C}$	$\tilde{\mathbf{C}}$	ε
33^2	0.14	0.01	9.5	0.7	$4.3 \cdot 10^{-3}$
65^2	2.6	0.05	$1.4 \cdot 10^2$	3.5	$3.7 \cdot 10^{-3}$
129^2	——	0.24	nem	16	——
257^2	——	1	nem	64	——

TABLE 4. Computing time and storage cost, rank $k = 5$, $\text{cov}(x, y) = \exp\{-\rho\}$, $l_1 = l_2 = 1$, domain $\mathcal{G} = [0, 1]^2$.

can be applied for approximation of KLE [3]. Alternatively, one can apply low-rank tensor methods [2, 3] and reduce the computational cost to $\mathcal{O}(knd \log n)$, where $n = N^{1/d}$ number of degrees of freedom in one direction.

Conclusion: We have successfully applied the $\mathcal{H}$-matrix technique for the approximation of covariance matrices in 2D and 3D computational domains with non-trivial discretisation. The combination of the $\mathcal{H}$-matrix technique and iterative eigenvalue solvers are seen to be a very efficient way to compute the KLE.

REFERENCES

[1] B. N. Khoromskij, A. Litvinenko and H. G. Matthies, *Application of hierarchical matrices for computing the Karhunen-Loeve expansion*, Computing, **84** (2009), pp.49-67.

[2] B. N. Khoromskij and A. Litvinenko, *Data Sparse Computation of the Karhunen-Loeve Expansion*, AIP Conference Proceedings, Editors: Theodore E. Simos, George Psihoyios and Ch. Tsitouras, vol. 1048, num. 1, (2008), pp.311-314.

[3] W. Nowak, A. Litvinenko, *Kriging accelerated by orders of magnitude: combining low-rank covariance approximations with FFT-techniques*, accepted for publication in Mathematical Geosciences, (2013).

Numerical upscaling of eigenvalue problems
Axel Målqvist
(joint work with Daniel Peterseim)

1. Introduction

We present a numerical upscaling technique for computing eigenpairs of self-adjoint linear elliptic second order differential operators with arbitrary positive bounded coefficients. The precise setting is as follows. Let $\Omega \subset \mathbb{R}^d$ be a bounded Lipschitz domain with piecewise flat boundary and let $A \in L^\infty(\Omega, \mathbb{R}^{d \times d}_{\mathrm{sym}})$ be a matrix-valued coefficient with uniform spectral bounds. Consider the self-adjoint eigenvalue problem: find eigenpairs (u, λ) such that

$$(1) \qquad\qquad -\nabla \cdot (A \nabla u) = \lambda u.$$

A standard finite element approximation of these eigenvalues and eigenfunctions is constructed using a shape regular mesh $\mathcal{T}_h$ of Ω with a corresponding finite element space $V_h \subset V := H_0^1(\Omega)$: find eigenpairs $u_h^{(\ell)} \in V_h$ and $\lambda_h^{(\ell)} \in \mathbb{R}$ such that,

$$(2) \qquad a(u_h^{(\ell)}, v) := (A \nabla u_h^{(\ell)}, \nabla v) = \lambda_h^{(\ell)}(u_h^{(\ell)}, v), \quad \forall v \in V_h.$$

We are mainly interested in the small eigenvalues. Popular approaches for the computation of these eigenvalues include e.g. Lanczos/Arnoldi-type iterations or the QR-algorithm applied directly to the N_h-dimensional finite element matrices, where $N_h = \dim(V_h)$.

In our approach we avoid the application of an eigenvalue solver to the large-scale problem (2) directly. Instead, inspired by [3], we compute a low-dimensional approximation space $V_{\mathrm{cs}} \subset V_h$ first, with $N_H = \dim(V_{\mathrm{cs}}) \ll N_h$. This preprocessing step is done by (approximately) inverting the operator for special right hand sides and subject to certain linear constraints. Having performed N_H of those computations, the solution of a low-dimensional $N_H \times N_H$ eigenvalue problem by standard solvers yields approximations of the first N_H eigenpairs. The linear problems needed to be solved on the fine scale are totally independent.

Our method is related to some coarse finite element mesh with maximal width H. The accuracy of the approximate eigenvalues is expressed in terms of H. Without any assumptions on the smoothness of eigenfunctions, we prove that the error scales like H^4. Note that a standard first-order conforming finite element computation yields H^2 under full $H^2(\Omega)$ regularity, see e.g. [2]. Under such strong assumption the two-grid method [5] allows certain postprocessing (solution of linear problems on the fine scale) of the coarse finite element eigenpairs to increase the accuracy to H^4. This is also possible to exploit for our proposed method to get even higher order convergence.

2. Galerkin approximation and main result

We let $\mathcal{T}_H$ denote an underlying coarse regular finite element mesh, with mesh function H defined by $H|_T = \mathrm{diam}(T) := H_T$ for all $T \in \mathcal{T}_H$. We denote the

interior nodes of the mesh $\mathcal{N}$. We let $V_H = \text{span}(\{\phi_x\}_{x \in \mathcal{N}})$ be a finite element space such that $V_H \subset V_h$.

We recall the Clément type interpolant $\mathcal{I}_H : V \to V_H$ presented in [1]. Let $\mathcal{I}_H v = \sum_{x \in \mathcal{N}} (\mathcal{I}_H v)(x) \phi_x$, where,

$$(\mathcal{I}_H v)(x) = \frac{(v, \phi_x)}{(1, \phi_x)},$$

for all $x \in \mathcal{N}$. The following approximation and stability property holds,

$$H_T^{-1} \|v - \mathcal{I}_H v\|_{L^2(T)} + \|\nabla(v - \mathcal{I}_H v)\|_{L^2(T)} \le C \|\nabla v\|_{L^2(\omega_T)}, \quad \forall v \in V,$$

where ω_T is the collection of elements in $\mathcal{T}$ overlapping T.

We are ready to present the decomposition of the space V_h into a coarse and a fine part. We let the fine scale space be defined by,

$$V_{\text{fs}} := \text{kernel } \mathcal{I}_H = \{v \in V_h : \mathcal{I}_H v = 0\},$$

and the coarse scale space by,

$$V_{\text{cs}} = \{v \in V_h : a(v, w) = 0, \text{ for all } w \in V_{\text{fs}}\}.$$

This yields an a-orthogonal split of the space $V_h = V_{\text{cs}} \oplus V_{\text{fs}}$. We note that $\dim(V_{\text{cs}}) = \dim(V_H) = |\mathcal{N}|$. In order to compute a basis for V_{cs} we solve $|\mathcal{N}|$ corrector problems: find $\psi_x \in V_{\text{fs}}$ such that,

$$a(\psi_x, v) = a(\phi_x, v), \quad \text{for all } v \in V_{\text{fs}},$$

and let $V_{\text{cs}} = \text{span}(\{\phi_x - \psi_x\}_{x \in \mathcal{N}})$. The Galekin approximation of equation (2) in the space V_{cs} reads: find $u_{\text{cs}}^{(\ell)} \in V_{\text{cs}}$ and $\lambda_{\text{cs}}^{(\ell)} \in \mathbb{R}$ such that,

$$a(u_{\text{cs}}^{(\ell)}, v) = \lambda_{\text{cs}}^{(\ell)}(u_{\text{cs}}^{(\ell)}, v), \quad v \in V_{\text{cs}}.$$

We now present an error bound for the approximate eigenvalues.

Theorem 1. *Let H be sufficiently small so that $H \le C \ell^{-1/4} \sqrt{\frac{\alpha}{\lambda_h^{(l)}}}$. Then it holds*

$$(3) \qquad \frac{\lambda_{cs}^{(\ell)} - \lambda_h^{(\ell)}}{\lambda_h^{(\ell)}} \le C\sqrt{\ell} \left(H\sqrt{\frac{\lambda_h^{(\ell)}}{\alpha}} \right)^4 \quad \text{for all } \ell = 1, \dots, |\mathcal{N}|,$$

for some constant C only depending on Ω and the shape regularity constant and with α being the lower spectral bound of A.

Remark 1. In [3] it is shown that $\phi_x - \psi_x$ decays exponentially (in the number of coarse elements) away from node x. This allows the use of truncated patches of size $H\log(H^{-1})$, with Dirichlet boundary conditions, rather than solving for ψ_x on the entire domain Ω. Theorem 1 holds also when using truncated domains.

3. Numerical example

Let $\Omega := (-1,1)^2 \setminus [0,1]^2$ be the L-shaped domain. Consider the constant scalar coefficient $A = 1$ and consider uniform coarse meshes with maximal mesh widths $\sqrt{2}H = 2^{-1}, \ldots, 2^{-4}$ of Ω. The reference mesh $\mathcal{T}_h$ has maximal mesh width $h = 2^{-7}/\sqrt{2}$. We consider a $P1$ conforming finite element approximation of the eigenvalues on the reference mesh $\mathcal{T}_h$ and compare these discrete eigenvalues $\lambda_h^{(\ell)}$ with coarse scale approximations depending on the coarse mesh size H.

Table 5 shows results for the case without truncation, i.e., all linear problems have been solved on the whole of Ω. For fixed ℓ, the rate of convergence of the

ℓ	$\lambda_h^{(\ell)}$	$e^{(\ell)}(1/2\sqrt{2})$	$e^{(\ell)}(1/4\sqrt{2})$	$e^{(\ell)}(1/8\sqrt{2})$	$e^{(\ell)}(1/16\sqrt{2})$
1	9.6436869	0.003494567	0.000034466	0.000000546	0.000000010
2	15.1989274	0.009621397	0.000079887	0.000000845	0.000000010
3	19.7421815	0.023813222	0.000213097	0.000002073	0.000000023
4	29.5281571	0.096910157	0.000724615	0.000006574	0.000000076
5	31.9265496	0.094454625	0.000874659	0.000009627	0.000000138
6	41.4922250	-	0.002395227	0.000019934	0.000000254
7	44.9604884	-	0.002443271	0.000019683	0.000000223
8	49.3631826	-	0.003651870	0.000028869	0.000000308
9	49.3655623	-	0.004266472	0.000032835	0.000000355
10	56.7389993	-	0.006863742	0.000055219	0.000000618

TABLE 5. Errors $e^{(\ell)}(H) =: \frac{\lambda_H^{(\ell)} - \lambda_h^{(\ell)}}{\lambda_h^{(\ell)}}$ for $\ell = 1, \ldots, 10$, constant coefficient $A = 1$, and various choices of the coarse mesh size H.

eigenvalue error $\lambda_H^{(\ell)} - \lambda_h^{(\ell)}$ in terms of H observed in Table 5 is between 6 and 7 which is even better than predicted in Theorem 1. For more elaborate numerical results we refer to [4].

References

[1] C. Carstensen, *Quasi-interpolation and a posteriori error analysis in finite element methods*, M2AN Math. Model. Numer. Anal., 33, (1999), 1187–1202.
[2] M. G. Larson, *A posteriori and a priori error analysis for finite element approximations of self-adjoint elliptic eigenvalue problems*, SIAM J. Numer. Anal., 38, (2000), 608–625.
[3] A. Målqvist and D. Peterseim, *Localization of elliptic multiscale problems*, preprint http://arxiv.org/abs/1110.0692.
[4] A. Målqvist and D. Peterseim, *Computation of eigenvalues by numerical upscaling*, preprint http://arxiv.org/abs/1212.0090.
[5] J. Xu and A. Zhou, *A two-grid discretization scheme for eigenvalue problems*, Math. Comp., 70, (2001), 17–25.

Generalized multiscale finite element method for the wave equation

Eric Chung

(joint work with Yalchin Efendiev, Wing Tat Leung)

Let $\Omega \subset \mathbb{R}^2$ be a bounded domain of two dimensions. The aim of the paper is to develop a new multiscale method for the following wave equation

$$(1) \qquad \frac{\partial^2 u}{\partial t^2} = \nabla \cdot (a\nabla u) + f \qquad \text{in} \quad \Omega$$

with the homogeneous Dirichlet boundary condition $u = 0$ on $\partial\Omega$. The function $f(x, t)$ is a given source. The problem (1) is also supplemented with the following initial conditions

$$u(x, 0) = g_0(x), \qquad u_t(x, 0) = g_1(x).$$

We assume that the coefficient $a(x)$ is highly oscillatory, representing the complicated model in which the waves are simulated. It is well-known that solving (1) by standard methods requires a very fine mesh, which is computationally prohibited. Thus a coarse grid solver is needed.

Now, we will give a detailed description of our new generalized multiscale finite element method, following the general framework in [2]. The method gives a numerical solver on coarse grid, providing an efficient way to simulate waves in complicated media. As we will discuss next, the local basis functions are obtained via the solutions of some local spectral problems. The POD technique is then used to obtain the most dominant modes. These modes form the basis functions of our multiscale finite element method.

Let V_h be the standard finite element space on the fine mesh. We introduce a coarse mesh that consists of union of connected fine-mesh grid blocks and is denoted by $\mathcal{T}^H$ and the set of all edges is denoted by $\mathcal{E}^H$. We denote the size of the coarse mesh by H. Next, we define the snapshot space. Let X_h be the space of conforming multiscale basis functions with respect to the coarse grid $\mathcal{T}^H$. More precisely, an element in X_h is obtained by solving $\nabla \cdot (a\nabla u) = 0$ in each coarse grid block with piecewise linear boundary conditions. The the coarse space V_H is obtained by solving an eigenvalue problem on X_h locally on each coarse block.

We can then state the IPDG method [1] as: find $u_H(t, \cdot) \in V_H$ such that

$$(2) \qquad (\frac{\partial u_H}{\partial t^2}, v) + a_{DG}(u_H, v) = l(v), \qquad \forall v \in V_H,$$

where the bilinear form $a_{DG}(u, v)$ and the linear functional $l(v)$ are defined by

$$a_{DG}(u, v) = \sum_{K \in \mathcal{T}^H} \int_K a\nabla u \cdot \nabla v$$

$$+ \sum_{e \in \mathcal{E}^H} \left(- \int_e \{a\nabla u \cdot n\}_e \, [v]_e - \int_e \{a\nabla v \cdot n\}_e \, [u]_e + \frac{\gamma}{H} \int_e a[u]_e \, [v]_e \right)$$

$$l(v) = (F, v) - a_{DG}(p_h, v)$$

where $\gamma > 0$ is a penalty parameter and n denotes the unit normal vector on e. A related DG method for high contrast flow problem is developed in [3].

Next, we will present a numerical example of using the above method when $a(x)$ is the Marmousi model. The computational results are shown in TABLE 6. In the table, we present the results of using all basis functions (using all energy), a subset of basis functions with 5% and 10% of the total energy. The relative L^2 error and relative L^2 error for cell averages are denoted by e_2 and $\overline{e_2}$. The time for offline and online computations are denoted by t_m and t_l respectively. The computation time for fine mesh solution is 4.58. From the table, we see that our method provides a significant speed up for a reasonable level of error.

E	num of basis	e_2	$\overline{e_2}$	t_m	t_l
0.05*total E	9	0.0665	0.0553	14.878059	0.129203
0.1*total E	12	0.0508	0.0379	32.922124	0.181453
total E	32	0.0444	0.0308	1057.213370	1.170797

TABLE 6. Result with POD for Marmousi.

REFERENCES

[1] E. Chung and W. Leung, *A sub-grid structure enhanced discontinuous Galerkin method for multiscale diffusion and convection-diffusion problems*, Commun. Comput. Phys., 14 (2013), pp. 370-392.
[2] Y. Efendiev, J. Galvis and T. Hou, *Generalized multiscale finite element mehthod*, Submitted.
[3] Y. Efendiev, J. Galvis, R. Lazarov, M. Moon and M. Sarkis, *Generalized multiscale finite element mehthod. Symmetric interior penalty coupling*, Submitted.

The localized reduced basis multi-scale method with online enrichment

FELIX ALBRECHT

(joint work with Mario Ohlberger)

We are interested in the efficient and reliable numerical solution of parametric multi-scale problems, the multi-scale (parametric) character of which is indicated by $\varepsilon\,(\mu)$ if expressed in the general notation of (1). It is well known that solving parametric multi-scale problems accurately can be challenging and computationally costly for small scales ε and for a strong dependency of the solution on μ.

Two traditional approaches exist to reduce this computational complexity: numerical multi-scale methods and model order reduction techniques. Numerical multi-scale methods reduce the complexity of multi-scale problems with respect to ε, while model order reduction techniques reduce the complexity of parametric problems with respect to μ (for both see [3] and references therein).

The localized reduced basis multiscale (LRBMS) method is a combination of both to reduce the complexity of parametric multi-scale problems with respect to ε and μ simultaneously. It performs well, for instance in the context of two-phase

flow problems (see [1]), but still requires solving (1) on the ε scale for several parameters μ, just like classical RB methods. Therefore, we propose an extension to the LRBMS method which requires a smaller number of full solutions of (1) by further incorporating localization ideas from numerical multi-scale methods.

Following the notation of [3], we consider solutions $_\mu^\varepsilon u_h \in U_h$ of the parameterized variational multi-scale problem

$$(1) \qquad\qquad R_\mu^\varepsilon[_\mu^\varepsilon u_h](v_h) = 0 \qquad\qquad \forall v_h \in V_h,$$

with trial and test function spaces $U_h, V_h : \Omega \subset \mathbb{R}^d \to \mathbb{R}$, $d = 1, 2, 3$, and an ε- and μ-dependent mapping $R_\mu^\varepsilon : U_h \to V_h'$. The approximation spaces U_h and V_h are associated with a fine triangulation τ_h of Ω resolving the ε scale.

In general, numerical multi-scale methods capture the macroscopic behavior of the solution in coarse approximation spaces, e.g., $V_H \subset V_h$, usually associated with a coarse triangulation $\mathcal{T}_H$ of Ω, and recover the microscopic behavior of the solution by local fine-scale corrections. Inserting this additive decomposition into (1) yields a coupled system of a fine- and a coarse-scale variational problem. By appropriately selecting trial and test spaces and defining the localization operators to decouple this system, a variety of numerical multi-scale methods can be recovered, e.g., the multi-scale finite element method, the variational multi-scale method and the heterogeneous multi-scale method (see [3] and references therein).

Model order reduction using reduced basis (RB) methods, on the other hand, is based on the idea to introduce a reduced space $V_{\text{red}} \subset V_h$, spanned by solutions of (1) for a limited number of parameters μ. These training parameters are iteratively selected by an adaptive greedy procedure. Depending on the choice of the training parameters and the nature of the problem V_{red} is expected to be of a significantly smaller dimension than V_h. Additionally, if R_μ^ε allows for an affine decomposition with respect to μ, its components can be projected onto V_{red}, which can then be used to effectively split the computation into an offline and online part (see [1, 3]). In the offline phase all parameter-independent quantities are precomputed, such that the online phase's complexity only depends on V_{red}.

The idea of the combined LRBMS approach, for $U_h = V_h$, is to generate a local reduced space $V_{\text{red}}^T \subset V_h^T$ for each coarse element of $\mathcal{T}_H$, given a tensor product type decomposition of the fine approximation spaces, $V_h = \oplus_{T \in \mathcal{T}_H} V_h^T$. The coarse reduced space is then given as $V_{H,\text{red}} := \oplus_{T \in \mathcal{T}_H} V_{\text{red}}^T \subset V_h$, resulting in a multiplicative decomposition of the solution into $_\mu^\varepsilon u_{H,\text{red}}(x) = \sum_{i=1}^{\dim(V_{H,\text{red}})} u_i^\mu(x)\varphi_i^\varepsilon(x)$, where the reduced basis functions φ_i^ε capture the microscopic behaviour of the solution and the coefficient functions u_i^μ only vary on the coarse triangulation.

We detail the LRBMS method in the context of linear elliptic parametric multi-scale problems, which arise for instance as the pressure equation in the two-phase flow context: : find $_\mu^\varepsilon u_h \in V_h$, such that $-\nabla \cdot (a_\mu^\varepsilon \nabla\, _\mu^\varepsilon u_h) = f_u$ holds in a weak sense with homgeneous dirichlet boundary conditions. In this context, the residual in

(1) is given as $R^\varepsilon_\mu[\cdot] := {}^\varepsilon_\mu A[\cdot] - F_\mu$, where ${}^\varepsilon_\mu A$ and F_μ can be expressed as

$$ {}^\varepsilon_\mu A[\cdot] = \sum_{T \in \mathcal{T}_H} {}^\varepsilon_\mu A^T[\cdot] + \sum_{T,S \in \mathcal{T}_H} {}^\varepsilon_\mu A^{T,S}[\cdot], \qquad F_\mu = \sum_{T \in \mathcal{T}_H} F^T_\mu, $$

where the coupling operators ${}^\varepsilon_\mu A^{T,S}$ are given as in the SWIP discontinuous galerkin context for any nontrivial combination of $T, S \in \mathcal{T}_H$ (see [1] for details). The local opearators and functionals ${}^\varepsilon_\mu A^T$ and F^T_μ can be given by any suitable discretization inside the coarse element T, for instance by a continuous finite element discretization in a local fine space V^T_h of piecewise linear polynomials on the fine triangulation inside the coarse element T. The local reduced spaces $V^T_{\mathrm{red}} := <\Phi^T>$ are then spanned by local reduced bases Φ^T which are computed by restricting and compressing global solution snapshots.

Here we propose an online enrichment step as an addition to the LRBMS method to reduce the need for global solution snapshots. While it is not feasible in the RB framework to compute solution snapshots during the online phase, the LRBMS frameworks allows us to carry out local computations in the online phase to enrich the local reduced bases. The idea of the LRBMS method with online enrichment is as follows: the initial construction of the local reduced bases is carried out as described above but using fewer training parameters and thus less global snapshots. Given local error indicators $\||{}^\varepsilon_\mu u_h|_T - {}^\varepsilon_\mu u_{H,\mathrm{red}}|_T\||_T \le \eta^T_{\mathrm{red}}({}^\varepsilon_\mu u_{H,\mathrm{red}})$ we efficiently asses the quality of the reduced solution ${}^\varepsilon_\mu u_{H,\mathrm{red}} \in V_{H,\mathrm{red}}$ with respect to the reference solution ${}^\varepsilon_\mu u_h \in V_h$ during the online phase and select coarse elements $\hat{\mathcal{T}}_H \subseteq \mathcal{T}_H$ where the local reduced bases are insufficient for the current parameter μ. In a local offline phase we compute a local correction function $\varphi^{T^\delta}_{\mathrm{cor}} \in V^{T^\delta}_h$ for each $T \in \hat{\mathcal{T}}_H$ on an oversampled domain $T \subset T^\delta$ by solving

$$ {}^\varepsilon_\mu A^{T^\delta}[\varphi^{T^\delta}_{\mathrm{cor}}](v_h) = F^{T^\delta}_\mu(v_h) - {}^\varepsilon_\mu A^{T^\delta}[{}^\varepsilon_\mu u_{H,\mathrm{red}}|_{T^\delta}](v_h) \qquad \forall v_h \in V^{T^\delta}_h. $$

We then restrict this correction function to T and enrich the existing local reduced basis on T by adding $\varphi^{T^\delta}_{\mathrm{cor}}|_T$ after orthonormalization. This process is repeated until the quality of the reduced solution meets the prescribed torelance again. After this local offline phase all quantities are made available in a reduced fashion again and the online phase continues. We repeat this process for each parameter, which is not yet captured by the local reduced bases.

We exemplify the local offline phase by a 2d thermalblock problem, illustrated in figure 1, where the local reduced bases have been trained in the offline phase with one global solution snapshot to μ_{train}, computed on a fine triangulation τ_h with 2500 elements utilizing the discretiation framework `Dune-Fem` [2]. During the online phase we solve for a test parameter μ_{test} which only differs from μ_{train} locally in T_0 and T_2. Since the reduced basis is insufficient for μ_{test}, a local offline phase is started to enrich the local bases until the indicated errors fall below $5e^{-4}$ (figure 1, right). As indicators η^T_{red} we use the true relative error in the local energy norm. For a local oversampling size of ten for example (red line, circular markers), the error torelance is reached after 14 iterations. The resulting sizes of the local

reduced bases, $(|\Phi^0|, |\Phi^1|, |\Phi^2|, |\Phi^3|) = (14, 6, 14, 6)$, show the local influence of the parameter component μ_2 and the symmetry of the problem (figure 1, left).
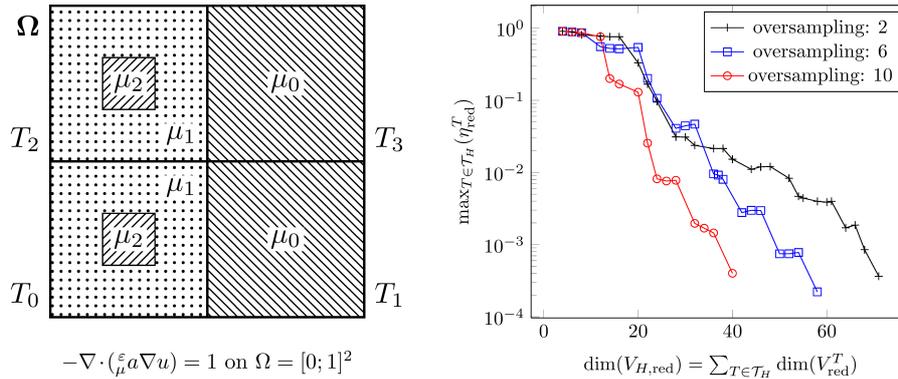
FIGURE 1. Thermalblock example with the values of the piecewise constant parametric diffusion $\frac{\varepsilon}{\mu}a$ given by $\mu = (\mu_0, \mu_1, \mu_2)'$ and the coarse triangulation $\mathcal{T}_H = \cup_{i=0}^3 T_i$ (left). Error evolution during the local offline phase (right): maximum local relative error for $\mu_{\text{test}} = (0.1, 1, 0.01)'$ against size of the coarse reduced space with the local reduced bases trained only with $\mu_{\text{train}} = (0.1, 1, 1)'$ for several sizes of oversampling layers (colored).

REFERENCES

[1] F. Albrecht, B. Haasdonk, S. Kaulmann and M. Ohlberger, *The Localized Reduced Basis Multiscale Method*, In A. Handlovičová and Z. Minarechová and D. Ševčovič (editor(s)): ALGORITMY **2012** - Proceedings of contributed papers and posters (2012), 393–403

[2] A. Dedner, R. Klöfkorn, M. Nolte and M. Ohlberger, *A generic interface for parallel and adaptive discretization schemes: abstraction principles and the Dune-Fem module*, Computing **90(3-4)**, (2010), 165–196

[3] M. Ohlberger., *Error control based model reduction for multi-scale problems.*, In A. Handlovičová and Z. Minarechová and D. Ševčovič (editor(s)): ALGORITMY **2012** - Proceedings of contributed papers and posters (2012), 1–10

Robust Multilevel Schwarz Methods for Multiscale Problems
JÖRG WILLEMS

In this talk we focus on the development of robust multilevel Schwarz solvers for symmetric positive definite (SPD) systems resulting from the discretization of partial differential equations (PDEs) with highly varying or otherwise degenerate coefficients. Particular emphasis is put on the case when coefficient variations are neither periodic nor statistically homogeneous but exhibit pronounced non-local features.

The three systems of equations under consideration are the stationary diffusion equation, the equations of linear elasticity for an isotropic medium, and the curl-curl equation with positive L^2-term:

$$(1) \qquad \text{(stationary diffusion)} \qquad -\nabla \cdot (K\nabla u) = f$$

with u denoting the concentration, $K = [K_{i,j}]_{i,j=1}^d$ the SPD permeability tensor, and f a volumetric source;

$$(2) \qquad \text{(linear elasticity)} \qquad -\nabla \cdot (\eta_1(\nabla \cdot \boldsymbol{u})I + 2\eta_2\varepsilon(\boldsymbol{u})) = \boldsymbol{f}$$

where $\boldsymbol{u}$ is the displacement, η_1, η_2 the Lamé parameters, I the identity matrix, and $\boldsymbol{f}$ the volumetric force;

$$(3) \qquad \text{(curl-curl)} \qquad \nabla \times (\mu^{-1}\nabla \times \boldsymbol{u}) + \kappa\boldsymbol{u} = \boldsymbol{f},$$

here $\boldsymbol{u}$ denotes the vector potential, μ is the permeability, and κ is real and positive. (3) e.g. arises in the solution of the instationary Maxwell's equations when employing implicit time stepping schemes.

Multiplying (1), (2), and (3), respectively, by suitable test functions, performing integration by parts, and assuming proper boundary conditions leads to variational problems of the following form:

Find $u \in V$ such that for all $v \in V$ we have $a_\Omega(u, v) = F(v)$,

where V is a suitable (infinite dimensional) function space, $F \in V'$ is a bounded linear functional and $a_\Omega(\cdot, \cdot)$ is a bounded SPD bilinear form on $V \times V$. For a finite dimensional subspace $V_h \subset V$ we consider the discrete variational formulation:

$$(4) \qquad \text{Find } u_h \in V_h \text{ such that for all } v_h \in V_h \text{ we have } a_\Omega(u_h, v_h) = F(v_h).$$

We focus on the development and analysis of efficient and robust multilevel solvers for (4) (see also [6, 8, 9] and the references therein and also [3, 4, 5, 7, 10] for recent advances in this area of research).

The abstract framework that we discuss in this talk relies on the construction of a sequence of increasingly coarser spaces ranging from the finest level L to the coarsest level 0, i.e.,

$$(5) \qquad V_0 \subset V_1 \subset \ldots \subset V_l \subset V_{l+1} \subset \ldots \subset V_{L-1} \subset V_L := V_h.$$

Let $\{\Omega_{l,j}\}_{j=1}^{n_l}$ be a family of overlapping subdomains, then V_l is constructed in such a way that for each $v_{l+1} \in V_{l+1}$ there exist $(v_{l+1,0} :=)v_l \in V_l$ and $v_{l+1,j} \in V_{l+1}^0(\Omega_{l,j}) := \{v \in V_{l+1} \,|\, \mathrm{supp}(v) \subset \Omega_{l,j}\}$, $j = 1, \ldots, n_l$ satisfying

$$(6) \qquad v_{l+1} = \sum_{j=0}^{n_l} v_{l+1,j} \qquad \text{and} \qquad \sum_{j=0}^{n_l} \|v_{l+1,j}\|_a^2 \leq C\|v_{l+1}\|_a^2,$$

where $\|\cdot\|_a$ is the norm induced by $a_\Omega(\cdot, \cdot)$ and C is a constant independent of problem and mesh parameters. (6) is the well-known stable decomposition property playing a prominent role in the analysis of overlapping Schwarz domain decomposition methods (cf. e.g. [6, Section 2.5]).

The inequality in (6) can be achieved with a robust constant C if V_l is constructed in the following way (see [1, 3, 10]): Let $\{\Xi_{l,j}\}_{j=1}^{n_l}$ be a partition of identity corresponding to $\{\Omega_{l,j}\}_j^{n_l}$, i.e.,

$$\Xi_{l,j} : V_{l+1} \to V_{l+1}^0(\Omega_{l,j}) \qquad \text{and} \qquad \sum_{j=1}^{n_l} \Xi_{l,j} = I,$$

where I denotes the identity operator. Assuming that for any $j = 1, \ldots, n_l$ and any $v_{l+1}, w_{l+1} \in V_{l+1}$ with $v_{l+1}|_{\Omega_{l,j}} \equiv w_{l+1}|_{\Omega_{l,j}}$ it holds that $\Xi_{l,j} v_{l+1} \equiv \Xi_{l,j} w_{l+1}$ we may with a slight abuse of notation but without any ambiguity write

$$\Xi_{l,j} : V_{l+1}(\Omega_{l,j}) := V_{l+1}|_{\Omega_{l,j}} \to V_{l+1}^0(\Omega_{l,j}) \qquad \text{with} \qquad \Xi_{l,j}(v_{l+1}|_{\Omega_{l,j}}) := \Xi_{l,j} v_{l+1}.$$

Now, for $j = 1, \ldots, n_l$ let $m_{\Omega_{l,j}}(\cdot, \cdot) : V_{l+1}(\Omega_{l,j}) \times V_{l+1}(\Omega_{l,j}) \to \mathbb{R}$ be an SPD bilinear form satisfying $\|\Xi_{l,j} v_{l+1}\|_a \leq \|v_{l+1}|_{\Omega_{l,j}}\|_{m,\Omega_{l,j}}$, where $\|\cdot\|_{m,\Omega_{l,j}}$ is the norm induced by $m_{\Omega_{l,j}}(\cdot, \cdot)$. With this notation we consider the following local generalized eigenvalue problems: Find $(\lambda_{l+1,j}^i, \varphi_{l+1,j}^i) \in (\mathbb{R}_0^+, V_{l+1}(\Omega_{l,j}))$ such that

$$a_{\Omega_{l,j}}(w, \varphi_{l+1,j}^i) = \lambda_{l+1,j}^i \, m_{\Omega_{l,j}}(w, \varphi_{l+1,j}^i), \quad \forall w \in V_{l+1}(\Omega_{l,j}),$$

where $a_{\Omega_{l,j}}(\cdot, \cdot)$ indicates that $a_\Omega(\cdot, \cdot)$ is restricted to the subset $\Omega_{l,j} \subset \Omega$. Then, for an arbitrarily chosen threshold τ_λ^{-1} and $w \in V_{l+1}(\Omega_{l,j})$ it holds with $P_{\Omega_{l,j}}^a w := \sum_{i : \lambda_{l+1,j}^i < \tau_\lambda^{-1}} a_{\Omega_{l,j}}(w, \varphi_{l+1,j}^i) \varphi_{l+1,j}^i$ that (see e.g. [2, 4])

$$\|w - P_{\Omega_{l,j}}^a w\|_{m,\Omega_{l,j}}^2 \leq \tau_\lambda |w - P_{\Omega_{l,j}}^a w|_{a,\Omega_{l,j}}^2 \leq \tau_\lambda |w|_{a,\Omega_{l,j}}^2,$$

where $|\cdot|_{a,\Omega_{l,j}}$ is the semi-norm induced by $a_{\Omega_{l,j}}(\cdot, \cdot)$ on $V_{l+1}(\Omega_{l,j})$. The next coarser space $V_l \subset V_{l+1}$ is then defined as

$$V_l := \text{span}\left\{\Xi_{l,j} \varphi_{l+1,j}^i \,\middle|\, j = 1, \ldots, n_l \text{ and } i \text{ such that } \lambda_{l+1,j}^i < \tau_\lambda^{-1}\right\},$$

and it can be shown (cf. [3, 2, 4, 10]) that with a sequence of increasingly coarser spaces constructed in this way (6) holds with $C = C(\tau_\lambda) = \mathcal{O}(\tau_\lambda)$. Thus, it follows by standard arguments from the analysis of abstract Schwarz methods that the energy-norm of the error propagation operator of the (scaled) symmetric two-level hybrid Schwarz preconditioner satisfies $\|(I - \theta \sum_{j=1}^{n_l} \pi_{l+1,j})(I - \pi_l)(I - \theta \sum_{j=1}^{n_l} \pi_{l+1,j})\|_a < \delta$, where $\delta < 1$ depends only on the constant $C = C(\tau_\lambda)$ in (6), θ is a suitable scaling factor depending on the choice of the subdomains, and $\pi_{l+1,j}$ and π_l denote the $a_\Omega(\cdot, \cdot)$-orthogonal projections onto $V_{l+1}^0(\Omega_{l,j})$ and V_l, respectively.

It is straightforward to see that the error propagation operator of the hybrid Schwarz preconditioner can be interpreted as the error propagation operator of a two-grid method with (scaled) block Jacobi smoother and a coarse solve with respect to V_l. In order to extend this two-level method to an actual multilevel algorithm one may approximate this solve with respect to V_l by a recursion of the rationale just described. In order for the obtained multilevel method to have a convergence rate independent of the number of levels L one can apply the general framework of (nonlinear) AMLI (cf. [9, 10] and the references therein for details).

On an abstract level the multilevel method outlined above and detailed in [10] has been shown to be applicable to (4) resulting from (1), (2), and (3), respectively.

In this talk we provide some numerical examples verifying the robustness of the method when applied to the isotropic and anisotropic diffusion equation with highly varying multiscale permeability fields. Obtaining comparable results also for the equations of linear elasticity as well as the curl-curl equation is the object of ongoing research. Further topics of investigation include the question of how to choose the partition of identity and the subdomains in such a way that the nested spaces in (5) exhibit large coarsening factors. Since the computation of local generalized eigenvalue problems is computationally expensive, we additionally consider it worth studying the possibilities to supersede their actual solution by considerations involving an analysis of the (multiscale) coefficients.

References

[1] V. Dolean, P. Hauret, F. Nataf, C. Pechstein, R. Scheichl, and N. Spillane. Abstract robust coarse spaces for systems of PDEs via generalized eigenproblems in the overlaps. Technical Report 2011-07, University of Linz, Institute of Computational Mathematics, 2011, (submitted).

[2] Y. Efendiev, J. Galvis, R. Lazarov, and J. Willems. Robust domain decomposition preconditioners for abstract symmetric positive definite bilinear forms. *ESAIM Math. Model. Numer. Anal.*, 46(5):1175–1199, 2012.

[3] Y. Efendiev, J. Galvis, and P.S. Vassilevski. Multiscale spectral AMGe solvers for high-contrast flow problems. Technical Report 2012-02, Institute for Scientific Computation, 2012.

[4] J. Galvis and Y. Efendiev. Domain decomposition preconditioners for multiscale flows in high-contrast media. *Multiscale Model. Simul.*, 8(4):1461–1483, 2010.

[5] J. Galvis and Y. Efendiev. Domain decomposition preconditioners for multiscale flows in high contrast media: reduced dimension coarse spaces. *Multiscale Model. Simul.*, 8(5):1621–1644, 2010.

[6] T.P.A. Mathew. *Domain Decomposition Methods for the Numerical Solution of Partial Differential Equations.* Lecture Notes in Computational Science and Engineering. Springer, Berlin Heidelberg, 2008.

[7] R. Scheichl, P.S. Vassilevski, and L.T. Zikatanov. Weak approximation properties of elliptic projections with functional constraints. *Multiscale Model. Simul.*, 9(4):1677–1699, 2011.

[8] A. Toselli and O. Widlund. *Domain Decomposition Methods – Algorithms and Theory.* Springer Series in Computational Mathematics. Springer, 2005.

[9] Panayot S. Vassilevski. *Multilevel block factorization preconditioners.* Springer, New York, 2008. Matrix-based analysis and algorithms for solving finite element equations.

[10] J. Willems. Robust multilevel methods for general symmetric positive definite operators. Technical Report RICAM-Report 2012-06, Radon Institute for Computational and Applied Mathematics, 2012, (submitted).

Numerical Upscaling By Spectral Element Agglomeration Coarsening
Panayot S. Vassilevski

Abstract

In this talk we present some recent results on the construction of coarse spaces with guaranteed approximation properties utilizing spectral element agglomeration AMG coarsening, which we refer to as ϱAMGe *numerical upscaling*. We demonstrate the quality of the ϱAMGe coarse spaces on the popular SPE10 dataset.

1. Problem description

Consider a s.p.d. sparse matrix A coming from a finite element discretization of an elliptic PDE posed on a domain $\Omega \subset \mathbb{R}^d$, (plane polygon, $d = 2$) (or polytope, $d = 3$). We use quasiuniform mesh $\mathcal{T}_h$ with mesh size h and respective finite element space V_h. Also, let $\mathcal{N}_h$ be the set of Lagrangian degrees of freedom, that in the case of piecewise (bi)linear finite element space V_h coincide with the vertices $\{\mathbf{x}_i\}$ of the elements in $\mathcal{T}_h$. The corresponding elliptic bilinear form reads

$$(1) \qquad a(u,\ \varphi) = \int_{\Omega} k(\mathbf{x}) \nabla u \cdot \nabla \varphi \, d\mathbf{x},$$

where $k = k(\mathbf{x})$ is a given positive coefficient. It may admit very large jumps in certain parts of Ω which are assumed resolved by the fine-grid triangulation $\mathcal{T}_h$,

We now summarize our spectral aggregation/element agglomeration based approach to construct accurate enough coarse spaces. We assume that a set $\mathcal{T}_H$ of non–overlapping agglomerated elements $\{T\}$ has been constructed. This means that each T is a (connected) union of fine–grid elements $\{\tau\}$. Let the characteristic mesh size (diameter of $T \in \mathcal{T}_H$) be of order H. We do not assume that H is comparable to the fine–grid mesh–size h. For each T, we assemble the local stiffness matrix A_T and the local weighted mass matrix G_T. They correspond to the respective integrals of the form

$$\sum_{\tau \subset T} \int_{\tau} k(\mathbf{x}) \nabla \varphi_j \cdot \nabla \varphi_i \, d\mathbf{x} \text{ and } \sum_{\tau \subset T} \int_{\tau} k(\mathbf{x}) \varphi_j \varphi_i \, d\mathbf{x},$$

for all basis functions φ_i, φ_j with support intersecting T. We also need the diagonal of A restricted to T, D_T.

In addition to the set $\mathcal{T}_H$ of agglomerated elements T, we assume that we have respective aggregates $\{\mathcal{A}_i\}_{i=1}^{n_A}$ where each $\mathcal{A} = \mathcal{A}_i$ is contained in some T. The set $\{\mathcal{A}_i\}$ provides a non–overlapping partition of the set $\mathcal{N}_h$ of fine–degrees of freedom.

1.1. **The construction of tentative prolongator.** We use the following construction. For each agglomerated element T, we solve the local generalized eigenvalue problem

$$(2) \qquad\qquad A_T \mathbf{q}_k = \overline{\lambda}_k D_T \mathbf{q}_k, \; k = 1, \, \ldots, \, n_T,$$

where n_T is the number of fine–degrees of freedom in T. By choosing the first m_T eigenvectors in the lower part of the spectrum of $D_T^{-1} A_T$ (based on a given tolerance $\theta \in (0, 1)$) we form the rectangular matrix $Q_T = [\mathbf{q}_1, \, \ldots, \, \mathbf{q}_{m_T}]$. Then, we extract the rows of Q_T with row–indices from the aggregate $\mathcal{A}$ (where $\mathcal{A} \subset T$) and form $Q_{\mathcal{A}}$. Finally, using SVD, we form a linearly independent set from the columns of $Q_{\mathcal{A}}$. The resulting matrix $\widehat{P}_{\mathcal{A}}$ has orthogonal (hence linearly independent) columns. The global tentative prolongator is simply the block-diagonal matrix

$$(3) \qquad\qquad \widehat{P} = \begin{bmatrix} \widehat{P}_{\mathcal{A}_1} & 0 & \ldots & 0 \\ 0 & \widehat{P}_{\mathcal{A}_2} & \ldots & 0 \\ 0 & 0 & \ddots & 0 \\ 0 & \ldots & 0 & \widehat{P}_{\mathcal{A}_{n_A}} \end{bmatrix}.$$

1.2. **The smoothed prolongator.** Based on the tentative interpolant $\widehat{P}$ and a matrix polynomial $S = s_\nu(b^{-1} D^{-1} A)$ ([2]), where D is the diagonal of A and b is such that $\|D^{-\frac{1}{2}} A D^{-\frac{1}{2}}\| \leq b = \mathcal{O}(1)$, and

$$(4) \qquad\qquad s_\nu(t) = (-1)^\nu \frac{1}{2\nu + 1} \frac{T_{2\nu+1}(\sqrt{t})}{\sqrt{t}},$$

($T_{2\nu+1}$ is the Chebyshev polynomial of degree $2\nu + 1$) we define the actual interpolation matrix P, i.e., we let $P = S\widehat{P}$ which has the property that it becomes stable in energy norm.

2. Some tests on the SPE10 dataset

The SPE10 data set is characterized with a 3D domain with dimensions $1200 \times 2200 \times 170$ units and it is divided into cells of size $20 \times 10 \times 2$ units. Thus, the fine-scale model in 3D has $60 \times 220 \times 85$ cells. We consider the 3D domain cut into 85 horizontal slices and we solve a 2D problem for each slice. The 2D domain has dimensions 1200×2200 units and it is divided into cells of size 20×10 resulting in a mesh with 60×220 elements (13200 fine-grid elements). The coefficient on each slice is a scalar represented by piecewise constant functions.

The prolongator smoother polynomial degree is $\nu = 3$.

The coarse space is built by the spectral SA-AMGe method defined in the preceding section. We use geometric agglomerates such that each coarse element is also a rectangle and it is a union of fine–grid rectangular elements. We have chosen $H = 12h$. The fine-grid degrees of freedom within each agglomerated element are used to form aggregates.

We denote by $A(k)$ the global stiffness matrix computed for coefficient k.
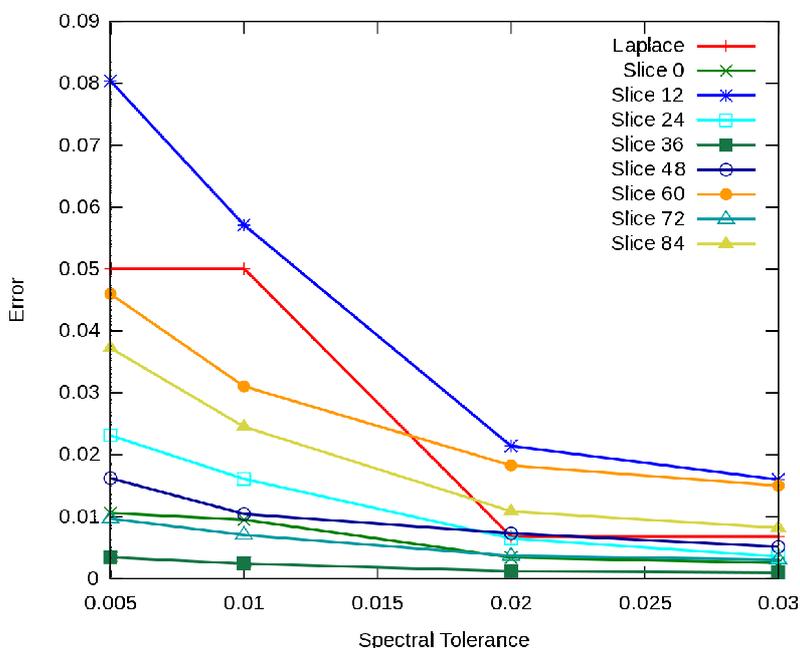
FIGURE 1. $\|\mathbf{u} - P\mathbf{u}_c\|_{A(k)}/\|\mathbf{u}\|_{A(k)}$ versus varying spectral tolerance θ (13481 fine dofs, 119641 non-zero elements of the fine-grid operator, 90 agglomerates).

For a given prolongator P and a stiffness matrix A we denote by $\mathbf{u}$ the computed (fine) solution of $A\mathbf{u} = \mathbf{f}$ and by $\mathbf{u}_c$ the computed (coarse) solution of $P^T A P\mathbf{u}_c = P^T\mathbf{f} = P^T A\mathbf{u}$. In Fig. 1, we show the relative energy error $\|\mathbf{u} - P\mathbf{u}_c\|_{A(k)}/\|\mathbf{u}\|_{A(k)}$ versus the spectral tolerance θ, or equivalently, versus the coarse dofs size.

REFERENCES

[1] M. Brezina and P. S. Vassilevski, "*Smoothed Aggregation Spectral Element Agglomeration AMG: SA-ρAMGe,*" In: Large-Scale Scientific Computing, "*8th International Conference, LSSC 2011, Sozopol, Bulgaria, June 6-10th, 2011. Revised Selected Papers,*" Lirkov, Ivan; Margenov, Svetozar; Wasniewski, Jerzy (Eds.), Lecture Notes in Computer Science, Vol. 7116, 2012, Springer, pp. 3-15. Available as Lawrence Livermore National Laboratory Technical Report LLNL-PROC-490083, June 29, 2011.

[2] M. BREZINA, P. VANĚK, AND P. S. VASSILEVSKI, "*An improved convergence analysis of smoothed aggregation algebraic multigrid,*" Numerical Linear Algebra with Applications **19**(3)(2012), pp. 441-469. Also available as Lawrence Livermore National Laboratory Technical Report LLNL-JRNL-448115, August 9, 2010.

Upscaling Approaches for Nonlinear Processes in Li-ion Batteries

Vasilena Taralova

(joint work with Yalchin Efendiev, Oleg Iliev)

Lithium-ion batteries are multiscale systems with complex porous structure on the microscale. A typical Li-ion battery consists of many electrically connected electrochemical cells. Each cell has two electrodes-anode and cathode. Both electrodes have porous structure consisting of connected active particles with the voids between them being filled with liquid electrolyte. We refer to the scale where we distinguish the porous structure of the electrodes as "microscale" and we denote the lengthscale of the whole electrode as "macroscale". We consider the isothermal model derived in [1]. On the microscopic scale nonlinear diffusion equations describe the transport of ions and charges in the active particles and in the electrolyte. Highly nonlinear interface conditions couple the equations in the two phases due to electrochemical reactions that occur on the boundary between the particles and the electrolyte. A detailed description of Li-ion batteries along with pictures is given in [3]. Depending on the type of the battery we can have a very big number of particles in each electrode. Therefore direct numerical simulations can be very computationally expensive. Our goal is to derive upscaled model on the lengthscale of the whole electrode which correctly captures the macroscopic behaviour of the electrodes and does not require resolving all the small-scale features. We consider periodically arranged particles and we rigorously derive coupled micro-macroscopic Li-ion battery model via the homogenization theory [4]. The equations of the electrolyte phase couple the concentration c^e of Li+ and the potential ϕ^e:

$$\text{(1a)} \qquad \frac{\partial c^e}{\partial t} - \nabla \cdot (k_{11}^e(c^e)\nabla c^e + k_{12}^e \nabla \phi^e) = 0, \quad x \in \Omega_e \subset \mathbb{R}^3$$

$$\text{(1b)} \qquad -\nabla \cdot (k_{21}^e(c^e)\nabla c^e + k_{22}^e \nabla \phi^e) = 0, \quad x \in \Omega_e \subset \mathbb{R}^3$$

where with Ω_e we denote the domain of the electrolyte. The equations describing the transport of Lithium ions and charge in the particles are

$$\text{(2a)} \qquad \frac{\partial c^s}{\partial t} - \nabla \cdot (D^s \nabla c^s) = 0, \quad x \in \Omega_s \subset \mathbb{R}^3$$

$$\text{(2b)} \qquad -\nabla \cdot (\kappa^s \nabla \phi^s) = 0, \quad x \in \Omega_s \subset \mathbb{R}^3$$

where Ω_s is the domain of the active (solid) particles, c^s is the concentration of Li+ in the particles, ϕ^s is the potential in the particles, D^s is the ion diffusion and κ^s is the electronic conductivity. We make no distinction between anode and cathode active particles since the equations describing the electrochemical processes in both types of particles are identical except for the values of the material parameters D^s and κ^s. The following interface conditions are imposed on the boundary between the active particles and the electrolyte:

$$\text{(3)} \qquad \mathbf{N}^s \cdot \mathbf{n_s} = \mathbf{N}^e \cdot \mathbf{n_s} = \mathcal{N}(c^e, c^s, \phi^e, \phi^s), \quad x \in \gamma$$

$$\text{(4)} \qquad \mathbf{J}^s \cdot \mathbf{n_s} = \mathbf{J}^e \cdot \mathbf{n_s} = \mathcal{J}(c^e, c^s, \phi^e, \phi^s), \quad x \in \gamma$$

where the ion flux and the electrical current in the electrolyte are respectively $\mathbf{N}^e = -(k_{11}^e(c^e)\nabla c^e + k_{12}^e\nabla\phi^e)$ and $\mathbf{J}^e = -(k_{21}^e(c^e)\nabla c^e + k_{22}^e\nabla\phi^e)$, and the ion flux and the electrical current in the particles are $\mathbf{N}^s = -D^s\nabla c^s$ and $\mathbf{J}^s = -\kappa^s\nabla\phi^s$. The unit normal vector $\mathbf{n_s}$ points in the direction from the particles to the electrolyte. With γ we denote the interface boundary between the solid and the electrolyte, and the current densities are $\mathcal{N} = \dfrac{k}{F}\sqrt{c^e c^s (c_{max}^s - c^s)}\left[\exp^{\frac{F\eta}{2RT}} - \exp^{\frac{-F\eta}{2RT}}\right]$ and $\mathcal{J} = F\mathcal{N}$ with $\eta = \phi^s - \phi^e - U_0(c^s)$. We consider periodic arrangement of the particles and as a single periodic cell we take a cubic block consisting of one active particle surrounded by electrolyte. If we denote with L the characteristic length of the electrodes and with l-that of the particles, for the small parameter $\varepsilon \to 0$ we take $\varepsilon = l/L$. Consequently the fast (microscopic) variable is $y = \dfrac{x}{\varepsilon}$, where x is the slow (macroscopic) variable. We denote the reference periodicity cell with Y (with characteristic size L), where $Y = E \cup S \cup \Gamma$ with E being the electrolyte domain in the reference cell, S-solid particle domain, and Γ-interface boundary between the electrolyte and the particle. The diffusion of Li+ in the particles is much slower than the diffusion of ions in the electrolyte. Therefore we do not upscale the equation for the concentration c^s of Li+ in the particles since the behaviour of the function c^s can be captured adequately only on the microscale. We pose equations (1) and (2b) in the whole domain Ω with the help of characteristic functions and then we perform the standard asymptotic analysis for $\varepsilon \to 0$. A crucial step in the correct homogenization of the model is the homogenization of the interface conditions. We show that the total flux across the whole interface boundary is preserved no matter how many active particles we have in the electrode. This is due to the fact that all the outer boundaries of the battery cell are insulated except for the cathode and anode boundaries where we apply constant potential and constant current respectively. This means that the total flux acroos the interface does not depend on ε. From here we obtain that the current densities $\mathcal{N}_\varepsilon$ and $\mathcal{J}_\varepsilon$ are of order ε. We rigorously upscale also the Neumann boundary conditions. Finally we obtain the following macroscopic equations for the homogenized concentration c_0^e and potentials ϕ_0^e and ϕ_0^s

(5a)
$$\frac{|E|}{|Y|}\frac{\partial c_0^e}{\partial t} - \nabla_x \cdot (\mathbf{K_{11}}\nabla_x c_0^e + \mathbf{K_{12}}\nabla_x \phi_0^e) = \frac{1}{\varepsilon\,|Y|}\int_\Gamma \mathcal{N}(c_0^e, c^s, \phi_0^e, \phi_0^s)\,ds, \quad x \in \Omega$$

(5b)
$$-\nabla_x \cdot (\mathbf{K_{21}}\nabla_x c_0^e + \mathbf{K_{22}}\nabla_x \phi_0^e) = \frac{1}{\varepsilon\,|Y|}\int_\Gamma \mathcal{J}(c_0^e, c^s, \phi_0^e, \phi_0^s)\,ds, \quad x \in \Omega$$

(5c)
$$-\nabla_x \cdot (\Lambda^s\nabla_x \phi_0^s) = -\frac{1}{\varepsilon\,|Y|}\int_\Gamma \mathcal{J}(c_0^e, c^s, \phi_0^e, \phi_0^s)\,ds, \quad x \in \Omega$$

where for each integration point $x \in \Omega$ we have to solve the following microscale problem for the concentration c^s of Li+ in the particles given in scale invariant

Potential in electrolyte

10 Particles, t=1, 20, 40, 80, 100 time steps, from bottom to top
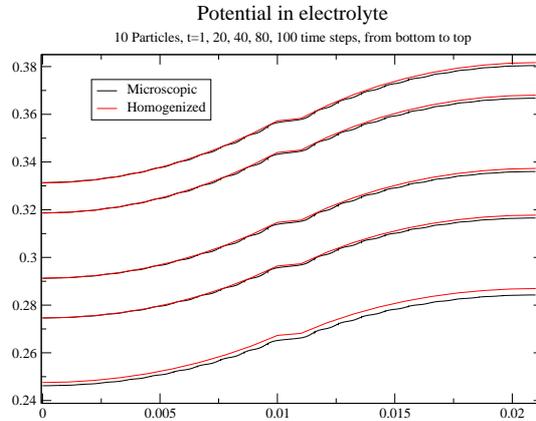
FIGURE 1. Homogenized and microscopic solution for $10 \times 10 \times 10$ particles in each electrode with $\varepsilon = 0.1$

form in terms of the variable $y \in S$

$$(6a) \qquad \frac{\partial c^s}{\partial t} - \nabla_y \cdot \left(\frac{D^s}{\varepsilon^2} \nabla_y c^s \right) = 0, \quad y \in S$$

$$(6b) \qquad -\frac{D^s}{\varepsilon^2} \nabla_y c^s \cdot \mathbf{n_s} = \frac{1}{\varepsilon} \mathcal{N}(c_0^e, c^s, \phi_0^e, \phi_0^s), \quad y \in \Gamma$$

We impose periodic boundary conditions on $\partial S \backslash \Gamma$, i.e. on the boundary of the solid particle where the particles are connected to each other. The coefficients in the homogenized equations (5) are nonlinear and they are tensors depending on the solutions of auxiliary cell problems which in our case are linear and do not depend on c_0^e, ϕ_0^e or ϕ_0^s. This means that the cell problems are solved only once. In Figure 1 we show numerical results for the potential ϕ^e. In [2] a similar approach is used to derive a macroscopic Li-ion battery model starting from a different microscopic model. However, there is no mathematical justification of the order of the current densities and no numerical results are shown.

REFERENCES

[1] A. Latz, J. Zausch, O. Iliev *Modeling of species and charge transport in Li-Ion batteries based on non-equilibrium thermodynamics*, Proceedings of the 7th international conference on Numerical methods and applications, **NMA'10** (2011), 329–337.
[2] W. Lai, F. Ciucci *Derivation of Micro/Macro Lithium Battery Models from Homogenization*, Transport in Porous Media **88** (2011), 249–270.
[3] M. Taralov, V. Taralova, P. Popov, O. Iliev, A. Latz, J. Zausch *Report on Finite Elements Simulations of Electrochemical Processes in Li-ion Batteries with Thermic Effects*, Berichte des Fraunhofer ITWM (2012).
[4] A. Bensoussan, J. L. Lions, G. Papanicolaou *Asymptotic Analysis for Periodic Structures*, North-Holland Publishing Company, (1978).

Global Model Reduction for Flows in High-Contrast Media

Michael Presho

(joint work with Yalchin Efendiev, Victor Calo, Mehdi Ghommem)

1. Introduction

In many porous media modeling applications the permeability of the media may vary over several orders of magnitude. For example, flow through a fractured porous medium is a scenario where the permeability within the fracture set may be significantly larger than in the surrounding medium. Similarly, shale barriers or deformation bands often represent regions whose permeability can be many orders of magnitude smaller than the surrounding regions. Both types of permeability variation can significantly affect the underlying flow dynamics, and the direct numerical simulation of these processes can be prohibitively expensive due to the small-scale effects of the respective configurations. In addition, the computational constraints are only magnified in situations where numerous simulations must be carried out for uncertainty quantification or sensitivity analysis. As a result, the use of reduced-order models that significantly reduce the number of degrees of freedom in the problem formulation are particularly desirable within this context.

Several techniques, including proper orthogonal decomposition (POD) and dynamic mode decomposition (DMD), have been used as effective reduced-order modeling techniques (see, e.g., [1, 2]). Both methods involve projecting the original set of equations into a reduced-dimension set of modal bases. However, the modes corresponding to each method are constructed in a different fashion. In particular, POD is a technique that attempts to extract the coherent structures of the underlying system by identifying the most energetic structures from a set of snapshots. In contrast, DMD hinges on the construction of modes resulting from a linear approximation of dynamically relevant structures. It should be noted that both methods enable the construction of a set of low-dimensional modes representing a linear or non-linear dynamical process. In this talk we apply both POD and DMD approaches to a flow model in highly heterogeneous porous media [3]. To test the performance of each approach we compute fully-resolved benchmark solutions and compare them with solutions sought within the respective modal approximation spaces. Aside from the relative success of both methods, DMD is shown to be a much more accurate global model reduction technique when Galerkin-projection is used to obtain the modal approximation.

2. Model equation

In this talk we consider the following parabolic equation that models single-phase porous media flow:

$$(1) \qquad \frac{\partial u}{\partial t} - \nabla \cdot \big(\kappa(x)\nabla u\big) = f(x) \quad \text{in } \Omega,$$

where Ω is a bounded domain, u is the pressure, f is an external forcing parameter, and $\kappa(x)$ is a high-contrast, isotropic permeability coefficient. In particular, the

ratio $\kappa_{\max}/\kappa_{\min}$ is assumed to be very large. A standard finite element discretization, and implicit time marching scheme yields matrix equations of the form

$$(2) \qquad U^{k+1} = \left(M + \Delta t A\right)^{-1} M U^k + \left(M + \Delta t A\right)^{-1} \Delta t F,$$

where $M_{ij} = \int_\Omega \phi_i \phi_j$ is a mass matrix, $A_{ij} = \int_\Omega \kappa \nabla \phi_i \cdot \nabla \phi_j$ is the stiffness matrix, $F_i = \int_\Omega f \phi_i$ is the forcing vector, and $U = [u_1, u_2, \ldots, u_n]^T$ is the unknown solution vector at each time step. We note that solutions from Eq. (2) will be used as the fully-resolved benchmarks for comparison with the mode decomposition techniques described next.

3. Mode decomposition methods

In this section we briefly describe the process of implementing proper orthogonal decomposition (POD) and dynamic mode decomposition (DMD). For POD we assume that a collection of solution "snapshots" is available in a matrix $V \in \mathbb{R}^{n \times m}$ where $m \ll n$:

$$V = \begin{bmatrix} v(t_1)\, v(t_2) \,\cdots\, v(t_m) \end{bmatrix}.$$

We then solve the $m \times m$ eigenvalue problem $V^* V X_i = \sigma_i^2 X_i$ in order to obtain the POD modes that are defined by

$$(3) \qquad \phi_i^{\mathrm{POD}} = \frac{1}{\sigma_i} V X_i.$$

For DMD we also assume that a sequence of snapshots written as

$$V_1^N = \{v_1, v_2, \ldots, v_N\},$$

is available. We note that the subscript of the snapshot matrix denotes the starting point of the snapshots, and the superscript denotes the end point of the snapshots. The main goal of DMD is to approximate the system dynamics by a linear mapping. That is, we wish to write

$$(4) \qquad V_1^N = \{v_1, A v_1, A^2 v_1, \ldots, A^{N-1} v_1\}.$$

For a sufficiently long sequence we assume that the solution at the Nth step may be written as $v_N = V_1^{N-1} a + r$, where $a = [a_1, a_2, \ldots, a_{N-1}]$ is an unknown coefficient vector, and r is the residual. Combining the above equation with (4) we may then write

$$A V_1^{N-1} = V_2^N = V_1^{N-1} S + r e_{N-1}^T,$$

where S is of the form

$$S = \begin{pmatrix} 0 & & & & a_1 \\ 1 & 0 & & & a_2 \\ & \ddots & \ddots & & \vdots \\ & & 1 & 0 & a_{N-2} \\ & & & 1 & a_{N-1} \end{pmatrix}.$$

In order to obtain the final form of the above matrix, we solve the minimization problem $S = \min_S \|V_2^N - V_1^{N-1} S\|$. We emphasize that S is the matrix that will be
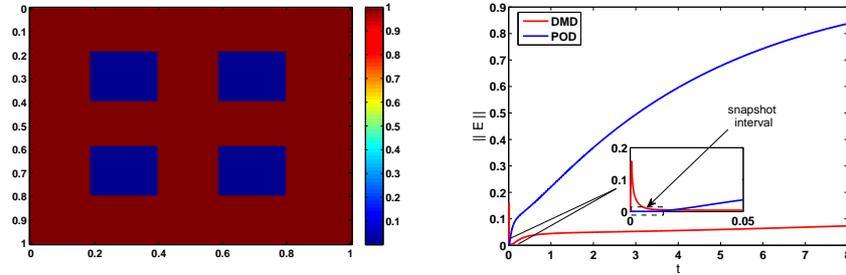
FIGURE 1. Illustration of a high-contrast field (left), and reduced-order model errors (right)

used to approximate the dynamics of the system. The solution of the minimization problem may be written as

$$S = \left((V_1^{N-1})^* \, V_1^{N-1}\right)^{-1} (V_1^{N-1})^* \, V_2^N,$$

although more robust forms are also available [2]. We then solve the eigenvalue problem $SX_i = \lambda_i X_i$, in order to compute the DMD modes given by

$$(5) \qquad\qquad\qquad \phi_i^{\mathrm{DMD}} = V_1^{N-1} X_i.$$

Then, using the modes from (3) or (5) we seek an approximate solution $u(x,t) \approx \widetilde{u}(x,t) = \sum_{i=1}^M \alpha_i(t)\phi_i(x)$ or $U^k \approx \widetilde{U}^k = \Phi\alpha^k$ and use the Galerkin projection

$$\left\langle \phi_i(x), \frac{\partial u}{\partial t} - \nabla \cdot \left(\kappa(x)\nabla u\right) - f \right\rangle = 0,$$

in order to obtain the following reduced-order model for the unknown modal coefficients

$$\frac{d\alpha}{dt} = -\left(\Phi^* M \Phi\right)^{-1}\Phi^* A \Phi \alpha + \left(\Phi^* M \Phi\right)^{-1}\Phi^* F.$$

In the talk, the performance of the above model is assessed by considering a variety of high-contrast permeability coefficients, and we offer a condensed set of results in Fig. 1. We see from the figure that DMD offers a more accurate and stable reduced-order model. We note that the results are representative of a variety of other permeability cases.

REFERENCES

[1] G. Berkooz, P. Holmes, J. L. Lumley, *The proper orthogonal decomposition in the analysis of turbulent flows*, Annual Review of Fluid Mechanics **53** (1993), 321–575.
[2] P. J. Schmid, *Dynamic mode decomposition of numerical and experimental data*, Journal of Fluid Mechanics **656** (2010), 5–28.
[3] M. Ghommem, V. Calo, Y. Efendiev, *Mode decomposition methods for flows in high-contrast porous media. Part I. Global approach*, Submitted to JCP.

Homogenization of High-Contrast Brinkman Flows

Donald Brown

(joint work with Guanglian Li, Yalchin Efendiev, Viktoria Savatorova)

Simulating porous media flows has a wide range of applications. Often, these applications involve many scales and multi physical processes. A useful tool in the analysis of such problems in that of homogenization. Which provides an averaged description as a tool for circumventing the need for complicated simulation of the fine scale features. In this talk, we present recent developments of homogenization techniques in the application of flows in porous media. We present the ideas for extending these techniques to high-contrast flows of Brinkman type [1]. In addition, these ideas are connected by the modeling of multiscale fluid-structure interaction problems by including slowly varying geometry into the coefficients of permeability [2, 3]. Future work, including extension to coupling to deformable media and Brinkman-Forchheimer models, are also discussed.

In modeling of highly-contrast porous media, the Brinkman model is often proposed [4]. In areas of low permeability the diffusive behavior of the Darcy model dominates. While in areas of high flow, a Stokesian model is more relevant. The Brinkman model allows the incorporation of both of these phenomena. By adding an inertial term to the Stokes equation to slow the flow in areas of low permeability or from the other view, adding a viscous term to the mixed Darcy formulation we obtain the high-contrast Brinkman model. The advantage of this model as opposed to the Stokes-Darcy systems is the circumventing of complex interface conditions known as the Beaver-Shaffman-Joseph interface conditions.

The homogenization of such a system is more natural because all the information about the geometry is contained the coefficients . The other advantage of using the Brinkman model is the model at certain scales is homogenization invariant. Note that if we are at the pore-scale Stokes model and we homogenize we arrive at a Darcy diffusion equation [2, 3]. However, as will be shown in the talk, the Brinkman model homogenizes to Brinkman. Yielding a stable Brinkman-to-Brinkman multiscale simulation platform.

We now state our main result presented in [1] and introduce the Brinkman equations explicitly. Letting ε denote the characteristic scales, δ be the contrast parameter, $p_\varepsilon, u_\varepsilon$ the fine-scale pressure and velocity, the fine-scale Brinkman equation is given by

(1a) $$\nabla p_\varepsilon - \Delta u_\varepsilon + \alpha_\varepsilon^\delta \left(\frac{x}{\varepsilon} \right) u_\varepsilon = f \text{ in } \Omega,$$

(1b) $$\text{div}(u_\varepsilon) = 0 \text{ in } \Omega \text{ , } u_\varepsilon \text{ on } \partial\Omega.$$

We assume periodic structure of the Brinkman coefficient $\alpha_\varepsilon^\delta$, using two-scale asymptotics, deriving cell equations, and estimating correctors as in [3] and references therein, we will arrive at the homogenized Brinkman equation

(2a) $$\nabla \bar{p} - \Delta \bar{u} + \alpha^* \bar{u} = f \text{ in } \Omega,$$

(2b) $$\text{div}(\bar{u}) = 0 \text{ in } \Omega \text{ , } \bar{u} = 0 \text{ on } \partial\Omega.$$

From the careful corrector estimates, we are able to obtain an understanding of the convergence relationship between scales and contrast, a fact that is often lost in theoretical two-scale convergence arguments.

The connection to FSI can be made by again applying it in the iterative FSI framework. If we assume the deformation of the Brinkman domain, periodicity will be broken and a two-scale slowly varying $\alpha(x, \frac{x}{\varepsilon})$ will arise. Future work includes advanced algorithms, numerical schemes, and the extension to nonlinear Forchheimer flow. The extension of these methods too nonlinear Forchheimer is of particular interest to incorporate non-Darcy effect. It is given by

$$(3a) \qquad \nabla p_\varepsilon - \Delta u_\varepsilon + \alpha_\varepsilon^\delta \left(\frac{x}{\varepsilon} \right) u_\varepsilon + \beta_\varepsilon^\delta \left(\frac{x}{\varepsilon} \right) |u_\varepsilon| u_\varepsilon = f \text{ in } \Omega,$$

$$(3b) \qquad \qquad \operatorname{div}(u_\varepsilon) = 0 \text{ in } \Omega \ , \ u_\varepsilon = 0 \text{ on } \partial\Omega.$$

Applying corrector techniques to the above equation may be difficult and new machinery may need to be developed.

References

[1] D. L. Brown , G. Li, Y. Efendiev, V.L. Savatorova, *Homogenization of Brinkman for High-Contrast Flows*, SIAM MMS (submitted)

[2] D. L. Brown , Y. Efendiev, P. Popov, *On Homogenization of Stokes Flow in Slowly Varying Media with Applications to Fluid-Structure Interaction* , Int J. Geomathematics, Volume 2, **2** (2011) 281-305.

[3] E. Marusic-Paloka, . and A. Mikelic, *An Error Estimate for Correctors in the Homogenization of the Stokes and Navier-Stokes Equations in a Porous Medium* Bollettino U.M.I, Volume 7 (1996) 661-671.

[4] O. Iliev, R. Lazarov, J. Willems, *Variational multiscale Finite Element Method for flows in highly porous media.* SIAM MMS, Volume 9.4 (2011) 1350-1372.

Multiscale Finite Volume Formulation for Compositional Flow in Heterogeneous Porous Media

HADI HAJIBEYGI

(joint work with Hamdi Tchelepi)

Recent advances in the multiscale finite volume (MSFV) framework for modeling subsurface flows include iterative improvement of locally conservative approximate solutions (See e.g. [1-4]). The cumulative effort lays a strength foundation for a next-generation reservoir simulation tool. The MSFV developments have focused on immiscible multiphase flows. Here, we extend the MSFV approach to compositional flows, whereby components partition across multiple fluid phases. For compositional displacements, the sequential-implicit strategy using the natural-variables formulation results in a nonsymmetric pressure equation with strong dependence on the phase distribution. We present a new multiscale formulation for nonlinear multi-component multiphase flow, with general mass transfer. Following Shank and Vestal [5], a symmetric pressure equation is obtained by adding the component mass-conservation equations (total mass balance). Also in contrast to the existing multiscale approaches, the transport equations are cast in

terms of the overall mass fraction. The new formulation is weakly sensitive to the appearance or disappearance of fluid phases. The coupling between the discrete equations of the flow and transport problems is performed in a consistent and locally conservative manner, and that allows one to terminate the iterations before tight residual tolerances are reached. This mass-conservative property is crucial for efficient modeling of compositional displacements in large heterogeneous reservoirs. Numerical examples are provided to validate the consistency of the proposed simulation strategy, and then to study the accuracy of the devised MSFV formulation.

REFERENCES

[1] P. Jenny, S. H. Lee, H. A. Tchelepi, Multi-scale finite-volume method for elliptic problems in subsurface flow simulation, Journal of Computational Physics, 187 (2003) 47-67.
[2] H. Zhou, Algebraic Multiscale Finite-Volume Methods for Reservoir Simulation, PhD dissertation, Stanford University, 2010.
[3] H. Hajibeygi, Iterative Multiscale Finite Volume Method for Multiphase Flow in Porous Media with Complex Physics, PhD dissertation, ETH Zurich, 2011. doi: 10.3929/ethz-a-006696714.
[4] Y. Wang, H. Hajibeygi, H. A. Tchelepi: Algebraic Multi-stage Multiscale Linear Solvers, Proceeding of The 13th European Conference on the Mathematics of Oil Recovery, 10 - 13 September, 2012, Biarritz, France.
[5] G. Shank and C. Vestal. Practical techniques in two-pseudocomponent black-oil simulation. SPE Reservoir Engineering, 4(2):244–252, 1989.

Generalized Multiscale Finite Element Methods

YALCHIN EFENDIEV

In this talk, we propose a general approach called Generalized Multiscale Finite Element Method (GMsFEM) for performing multiscale simulations for problems without scale separation over a complex input space. As in multiscale finite element methods (MsFEMs), the main idea of the proposed approach is to construct a small dimensional local solution space that can be used to generate efficient and accurate approximation to the multiscale solution with a potentially high dimensional input parameter space. In the proposed approach, we present a general procedure to construct the offline space that is used for a systematic enrichment of the coarse solution space in the online stage. The enrichment in the online stage is performed based on a spectral decomposition of the snapshot space consisting of all plausible functions in the space. In the online stage, for any input parameter, a multiscale space is constructed to solve the global problem on a coarse grid. The online space is constructed via a spectral decomposition of the offline space and by choosing the eigenvectors corresponding to the largest eigenvalues. In this talk, we discuss the use of oversampling and discontinuous Galerkin coupling mechanisms. The computational saving is due to the fact that the construction of the online multiscale space for any input parameter is fast and this space can be re-used for solving the forward problem with any forcing and boundary condition. Compared with the other approaches where global snapshots are used, the local approach that

we present in this paper allows us to eliminate unnecessary degrees of freedom on a coarse-grid level. We present various examples and some numerical results to demonstrate the effectiveness of our method.

MLMCMC – Multilevel Markov Chain Monte Carlo

ROBERT SCHEICHL

(joint work with Christian Ketelsen, Aretha Teckentrup, Panayot Vassilevski)

In this talk we address the problem of the prohibitively large computational cost of existing Markov chain Monte Carlo (MCMC) methods for large–scale applications with high dimensional parameter spaces, e.g. uncertainty quantification in porous media flow. We propose a new multilevel Metropolis-Hastings algorithm, and give an abstract, problem dependent theorem on the cost of the new multilevel estimator based on a set of simple, verifiable assumptions. For a typical model problem in subsurface flow, we then provide a detailed analysis of these assumptions and show significant gains over the standard Metropolis-Hastings estimator.

The parameters in mathematical models for many physical processes are often impossible to determine fully or accurately, and are hence subject to uncertainty. It is of great importance to quantify the uncertainty in the model outputs based on the (uncertain) information that is available on the model inputs. A popular way to achieve this is stochastic modelling. Based on the available information, a probability distribution (the *prior* in the Bayesian framework) is assigned to the input parameters. If in addition, some dynamic data (or *observations*) related to the model outputs are available, it is possible to reduce the overall uncertainty and to get a better representation of the model by conditioning the prior distribution on this data (leading to the *posterior*). In most situations, however, the posterior distribution is intractable in the sense that exact sampling from it is unavailable. One way to circumvent this problem, is to generate samples using a Metropolis–Hastings type MCMC approach [9], which consists of two main steps: (i) given the previous sample, a new sample is generated according to some proposal distribution, such as a random walk; (ii) the likelihood of this new sample (the data fit) is compared to the likelihood of the previous sample. Based on this comparison, the proposed sample is then either accepted and used for inference, or it is rejected and we use instead the previous sample again, leading to a Markov chain.

A major problem with MCMC is the high cost of the likelihood calculation for large-scale applications, since it commonly involves the numerical solution of a partial differential equation (PDE) with highly varying coefficients (for accuracy reasons usually) on a very fine spatial grid. Due to the slow convergence of Monte Carlo averaging, the number of samples is also large and moreover, the likelihood has to be calculated not only for the samples that are eventually used for inference, but also for the samples that end up being rejected. Altogether, this leads to an infeasibly high overall complexity, particularly in the context of high-dimensional parameter spaces, typical in realistic subsurface flow problems, where the acceptance rate of the algorithm can be very low.

We show here how the computational cost of the standard Metropolis-Hastings algorithm can be reduced significantly by using a multilevel approach. This has already proved highly successful in the context of standard Monte Carlo estimators based on independent and identically distributed (i.i.d.) samples [7, 5], in particular for subsurface flow problems [3, 1, 2, 10]. The basic ideas are to exploit the linearity of expectation, to introduce (in an unbiased way) a hierarchy of computational models that are assumed to converge (as the model resolution is increased) to some limit model (e.g. the original PDE), and to build estimators for differences of output quantities instead of estimators for the quantities themselves. In that way each individual estimator will either (i) have a smaller variance, since the differences of the output quantities from two consecutive models go to zero with increased model resolution, or (ii) require significantly less computational work per sample, if the model resolution is low. Either way the cost of an individual estimator is significantly reduced, easily compensating for the extra cost of having to compute L estimators instead of one, where L is the number of levels.

However, the application of the multilevel approach in the context of MCMC is not straightforward. The posterior distribution, which depends on the likelihood, has to be level-dependent, since otherwise the cost on all levels is dominated by the evaluation of the likelihood in the finest model leading to no real cost reduction on the coarser levels. Instead, and in order to avoid introducing extra bias in the estimator, we construct two parallel Markov chains $\{\theta_\ell^n\}_{n\geq 0}$ and $\{\Theta_{\ell-1}^n\}_{n\geq 0}$ on levels ℓ and $\ell - 1$ each from the correct posterior distribution on the respective level. The coarser of the two chains is constructed using the standard Metropolis–Hastings algorithm, for example using a (preconditioned) random walk. The main innovation is a new proposal distribution for the finer of the two chains $\{\theta_\ell^n\}_{n\geq 0}$. A similar two-level proposal distribution has been investigated before in [4], but only for standard single-level Metropolis-Hastings.

Let us describe the new algorithm for the following model problem of stationary, single phase flow in a porous medium:

$$(1) \qquad -\nabla \cdot (k(x,\omega)\nabla p(x,\omega)) = f(x), \qquad \text{in} \quad D \subset \mathbb{R}^d,$$

subject to the Dirichlet boundary condition $p(\omega, x) = p_0(x)$ on ∂D, with a lognormal distribution for the input random field, the permeability $k(x,\omega)$, with covariance function $C(x,y) = \sigma^2 \exp(-\|x-y\|_1/\lambda)$. We discretise (1) using standard, continuous, piecewise linear finite elements (FEs) on a sequence of grids $\{\mathcal{T}_\ell\}_{\ell\geq 1}$, with mesh width $h_\ell = h_0 2^{-\ell}$, and we sample from the input random field on level ℓ using a truncated Karhunen-Loève (KL) expansion of $\log k$,

$$(2) \qquad k_\ell(\theta_\ell(\omega), x) = \exp\Big(\sum_{j=1}^{R_\ell} \sqrt{\mu_j}\phi_j(x)\xi_j(\omega)\Big),$$

with R_ℓ terms. The KL-eigenpairs (μ_j, ϕ_j) are known explicitly for the above (exponential) covariance function $C(x,y)$. The prior of our model on level ℓ is thus the R_ℓ-dimensional random vector $\theta_\ell = (\xi_j)_{j=1}^{R_\ell}$ with multivariate standard normal $N(0, I)$ distribution $\mathcal{P}_\ell$. Using Bayes' Theorem, the posterior distribution,

conditioned on observations F_{obs} of some functional $\mathcal{F}(p)$ of the PDE solution, is

$$(3) \qquad \pi_\ell(\theta_\ell) = \mathbb{P}(\theta_\ell | F_{\text{obs}}) \propto \mathcal{L}_\ell(F_{\text{obs}} | \theta_\ell)\, \mathcal{P}_\ell(\theta_\ell).$$

with an (in general) intractable normalising constant $\mathcal{P}_F(F_{\text{obs}})$. The data fit is modelled to be Gaussian, i.e. $\mathcal{L}_\ell(F_{\text{obs}} | \theta_\ell) \propto \exp\left(-\|F_{\text{obs}} - \mathcal{F}(p_\ell(\theta_\ell))\|^2 / (2\sigma_F^2) \right)$, where p_ℓ is the PDE solution on $\mathcal{T}_\ell$ and σ_F^2 is the *fidelity*. The output quantity of interest is the expected value of another functional $Q = \mathcal{G}(p)$ of the PDE solution.

We start by choosing a tolerance $\varepsilon > 0$ and a grid $\mathcal{T}_L$, $L \in \mathbb{N}$, such that the bias $|\mathbb{E}_{\pi_L}[Q - Q_L]| \leq \varepsilon/\sqrt{2}$, where $Q_\ell = \mathcal{G}(p_\ell)$. Now, as indicated, we use linearity of expectation to define the following unbiased multilevel estimator for $\mathbb{E}_{\pi_L}[Q_L]$:

$$(4) \qquad \widehat{Q}_L^{\text{ML}} \;=\; \frac{1}{N_1} \sum_{n=1}^{N_1} Q_1(\theta_1^n) \;+\; \sum_{\ell=2}^{L} \frac{1}{N_\ell} \sum_{n=1}^{N_\ell} Q_\ell(\theta_\ell^n) - Q_\ell(\Theta_{\ell-1}^n).$$

The two Markov chains $\{\theta_\ell^n\}_{n\geq 0}$ and $\{\Theta_\ell^n\}_{n\geq 0}$, for $1 \leq \ell \leq L-1$, are independent, but drawn from the same posterior distribution π_ℓ. Clearly, the multilevel estimator coincides with the standard MCMC estimator on level L (in the limit as $N_1, \ldots, N_L \to \infty$), since all other terms cancel.

All the Markov chains $\{\theta_\ell^n\}_{n\geq 0}$ and $\{\Theta_\ell^n\}_{n\geq 0}$ in (4) are constructed via the following (standard) Metropolis-Hastings algorithm (for details see [9, 8]):

Algorithm 1. Choose θ^0 (from the prior $\mathcal{P}$ or from some "burnt-in" chain)

1. Given θ^n, generate a new proposal θ' from a proposal distribution $q(\theta'|\theta^n)$
2. Evaluate $\alpha(\theta'|\theta^n) = \min\left\{ 1, \dfrac{\pi(\theta')\, q(\theta^n|\theta')}{\pi(\theta^n)\, q(\theta'|\theta^n)} \right\}$.
3. Set $\theta^{n+1} = \begin{cases} \theta' & \text{with probability } \alpha(\theta'|\theta^n), \\ \theta^n & \text{with probability } 1 - \alpha(\theta'|\theta^n). \end{cases}$

In practice this is randomised by averaging over several such chains on each level. For the "coarse" chains $\{\theta_1^n\}$, $\{\Theta_1^n\}$, ..., $\{\Theta_{L-1}^n\}$ we use a standard proposal distribution $q = q_\ell^{\text{RW}}$ based on a preconditioned random walk [6].

The important new ingredient is a novel two-level proposal distribution $q = q_\ell^{\text{TL}}$ for the fine chains $\{\theta_2^n\}$, ..., $\{\theta_L^n\}$. We want the chains $\{\theta_\ell^n\}$ and $\{\Theta_{\ell-1}^n\}$ to be close, so that the variance of $Q_\ell(\theta_\ell^n) - Q_\ell(\Theta_{\ell-1}^n)$ is small and thus the variance of the estimator on level ℓ in (4) is small. To ensure this, we use $\theta_\ell' = [\Theta_{\ell-1}^{n+1}, \theta_{\ell,F}']$, where $\theta_{\ell,F}'$ contains the last $R_\ell - R_{\ell-1}$ ("fine") components of θ_ℓ' that are not active on level $\ell - 1$ and is obtained again by a random walk from $\theta_{\ell,F}^n$. It turns out that q_ℓ^{TL} is computable. It depends on the acceptance probability for $\Theta_{\ell-1}^{n+1}$, and so it follows via some algebra that the two-level acceptance probability is

$$(5) \qquad \alpha_\ell^{\text{TL}}(\theta_\ell'|\theta_\ell^n) = \min\left\{ 1, \frac{\pi_\ell(\theta_\ell')\ \pi^{\ell-1}(\theta_{\ell,C}^n)}{\pi_\ell(\theta_\ell^n)\pi^{\ell-1}(\Theta_{\ell-1}^{n+1})} \right\},$$

where $\theta_{\ell,C}^n$ denotes the first $R_{\ell-1}$ ("coarse") components of θ_ℓ^n.

For linear (or Fréchet differentiable) functionals $\mathcal{F}$ and $\mathcal{G}$ we have the following theoretical results. The first lemma is a consequence of the decay, as $j \to \infty$, of the KL-eigenvalues μ_j in (2).

Lemma 0.1 ([8, Theorem 4.6]). *Let* $R_\ell \gtrsim h_\ell^{-2}$. *Then all finite moments of* $1 - \alpha_\ell^{\mathrm{TL}}(\theta_\ell'|\theta_\ell)$ *are* $\mathcal{O}(h_{\ell-1}^{1-\delta})$, *for any* $\delta > 0$.

This means that on the finer levels we accept almost all samples. Using this together with the theory for standard Multilevel MC based on i.i.d. samples in [2, 10], it is possible to establish the following main result.

Theorem 0.1 ([8, Thm. 4.1 & 4.8]). *For any* ε, $\delta > 0$ *and* $\{\theta_\ell^0\}_{\ell=1}^L$ *with* $\pi_\ell(\theta_\ell^0) > 0$, *we have* $\lim_{\min\{N_\ell\}\to\infty} \widehat{Q}_L^{\mathrm{ML}} = \mathbb{E}_{\pi^L}[Q_L]$ *and there exists* $L \in \mathbb{N}$, $(N_\ell)_{\ell=1}^L \in \mathbb{N}^L$ *s.t.*

$$(6) \qquad \mathbb{E}_{\mathrm{ML}}\left[(\widehat{Q}_L^{\mathrm{ML}} - \mathbb{E}_{\pi^L}[Q])^2\right] \leq \varepsilon^2 \quad \text{and} \quad \mathrm{Cost}(\widehat{Q}_L^{\mathrm{ML}}) = \mathcal{O}(\varepsilon^{-(d+1)-\delta}),$$

where $\mathbb{E}_{\mathrm{ML}}[\cdot]$ *is expectation w.r.t. the joint distribution of all the chains in* (4).

Note that in comparison, the standard Metropolis-Hastings algorithm with q_L^{RW} instead of q_L^{TL} (but with the same L so that the bias is again less than $\varepsilon/\sqrt{2}$) has an ε-cost of $\mathcal{O}(\varepsilon^{-(d+2)-\delta})$, i.e. a whole power of ε more than the multilevel approach.

The numerical experiments for $d = 2$ in [8] confirm all these theoretical results. In fact, in practice it seems that (at least in the pre–asymptotic phase) the cost seems to grow only like $\mathcal{O}(\varepsilon^{-d})$ and the absolute cost is between 10 and 100 times lower than for the standard estimator, which is a vast improvement and brings the cost of the multilevel MCMC estimator down to a similar order than the cost of standard multilevel MC estimators based on i.i.d. samples. This provides real hope for practically relevant MCMC analyses for many large scale PDE applications.

Note also that there is nothing special about the model problem above and that the algorithm is applicable in any other MCMC application, provided the input parameters can be ordered according to their "importance" for the functionals $\mathcal{F}$ and $\mathcal{G}$. In [8, Theorem 3.5] we formulate the above theoretical results in abstract terms and show that under certain assumptions – that need to be verified for any new application – the multilevel estimator always leads to a reduction in the ε-cost over the standard Metropolis-Hastings algorithm.

References

[1] A Barth, C Schwab and N Zollinger, Multi–Level Monte Carlo finite element method for elliptic PDE's with stochastic coefficients, *Numer. Math.*, **119** (1):123–161, 2011.

[2] J Charrier, R Scheichl and AL Teckentrup, Finite element error analysis of elliptic PDEs with random coefficients and its application to multilevel Monte Carlo methods, *SIAM J. Num. Anal.*, **51** (1):322-352, 2013.

[3] KA Cliffe, MB Giles, R Scheichl and AL Teckentrup, Multilevel Monte Carlo methods and applications to elliptic PDEs with random coefficients, *Comput. Vis. Sci.*, **14**:3-15, 2011.

[4] Y Efendiev, T Hou and W Lou, Preconditioning Markov chain Monte Carlo simulations using coarse–scale models, *SIAM J. Sci. Comput.*, **28**(2):776–803, 2006.

[5] MB Giles, Multilevel Monte Carlo path simulation, *Oper. Res.*, **256** (3):981–986, 2008.

[6] M Hairer, AM Stuart and SJ Vollmer, Spectral gaps for a Metropolis–Hastings algorithm in infinite dimensions, preprint at `http://arxiv.org/abs/1112.1392`, submitted, 2011.

[7] S Heinrich, Multilevel Monte Carlo methods, in *Lecture Notes in Comput. Sci.*, Vol. 2179, Springer, pp. 3624-3651, 2001.

[8] C Ketelsen, R Scheichl, AL Teckentrup, A hierarchical multilevel Markov chain Monte Carlo algorithm with applications to uncertainty quantification in subsurface flow, submitted, 2013

[9] C Robert and G Casella, *Monte Carlo Statistical Methods*, Springer, New York, 1999.
[10] AL Teckentrup, R Scheichl, MB Giles and E Ullmann, Further analysis of multilevel MC methods for elliptic PDEs with random coefficients, *Numer. Math.*, publ. online March 2013.

Reporter: Michael Presho

Participants

Felix Albrecht
Institut für Numerische und
Angewandte Mathematik
Universität Münster
Orleans-Ring 10
48149 Münster
GERMANY

Dr. Donald Brown
King Abdullah University of Science
and Technology (KAUST)
Mathematical & Computer Sciences
UN 1500 Bldg. 1
P.O. Box 2360
Jeddah
SAUDI ARABIA

Prof. Dr. Eric T. Chung
Department of Mathematics
The Chinese University of Hong Kong
Shatin, Hong Kong N. T.
CHINA

Prof. Dr. Yalchin Efendiev
Department of Mathematics
Texas A&M University
TAMU 3368
College Station, TX 77843-3368
UNITED STATES

Dr. Hadi Hajibeygi
TU Delft
Civil Engineering & Geosciences
Dept. of Geoscience and Engineering
Stevinweg 1
2628 CN Delft
NETHERLANDS

Prof. Dr. Oleg Iliev
Fraunhofer Institute for Industrial
Mathematics
ITWM
Fraunhofer-Platz 1
67663 Kaiserslautern
GERMANY

Dr. Alexander Litvinenko
Institute of Scientific Computing
Technische Universität Braunschweig
Hans-Sommer-Str. 65
38106 Braunschweig
GERMANY

Prof. Dr. Yvon Maday
Université Pierre et Marie Curie
Laboratoire Jacques-Louis Lions
Boite courrier 187
4 place Jussieu
75252 Paris Cedex 05
FRANCE

Prof. Dr. Axel Malqvist
Dept. of Information Technology
Uppsala University
Box 337
75105 Uppsala
SWEDEN

Tigran Nagapetyan
Institut für Techno- und
Wirtschaftsmathematik e.V. (ITWM)
Fraunhofer-Platz 1
67663 Kaiserslautern
GERMANY

Dr. Michael P. Presho
Department of Mathematics
Texas A & M University
College Station, TX 77843-3368
UNITED STATES

Prof. Dr. Klaus Ritter
Fachbereich Mathematik
T.U. Kaiserslautern
Erwin-Schrödinger-Straße
67653 Kaiserslautern
GERMANY

Prof. Dr. Robert Scheichl
Dept. of Mathematical Sciences
University of Bath
Claverton Down
Bath BA2 7AY
UNITED KINGDOM

Dr. Vassilena Taralova
Institut für Techno- und
Wirtschaftsmathematik e.V. (ITWM)
Fraunhofer-Platz 1
67663 Kaiserslautern
GERMANY

Prof. Dr. Panayot S. Vassilevski
Center for Applied Scientific Computing
Lawrence Livermore National
Laboratory
P.O.Box 808, L-560
Livermore CA 94550
UNITED STATES

Dr. Jörg Willems
Johann Radon Institute for Comput.
and Applied Mathematics (RICAM)
Austrian Academy of Sciences
Altenbergerstr. 69
4040 Linz
AUSTRIA

Prof. Dr. Ludmil Zikatanov
Department of Mathematics
Pennsylvania State University
University Park, PA 16802
UNITED STATES